Master's Thesis of Science in Agriculture

PROKR1 delivery by cell-derived vesicles recovers the myogenic potency of C2C12$^{Prokr1-/-}$ cells

세포 유래 소포체를 이용한 PROKR1 전달을 통한 C2C12$^{Prokr1-/-}$ 세포의 근분화능 회복에 관한 연구

August 2020

Chunjuan Zhang

Department of International Agricultural Technology
Graduate School of International Agricultural Technology
Seoul National University

PROKR1 delivery by cell-derived vesicles recovers the myogenic potency of C2C12$^{Prokr1-/-}$ cells

A thesis
submitted in partial fulfillment of the requirements to the faculty
of Graduate School of International Agricultural Technology
for the Degree of Master of Science in Agriculture

By
Chunjuan Zhang

Supervised by
Prof. Joonghoon Park

Major of International Agricultural Technology
Department of International Agricultural Technology
Graduate School of International Agricultural Technology
Seoul National University

August 2020

Approved as a qualified thesis
for the Degree of Master of Science in Agriculture
by the committee members

Chairman **Tae Min Kim, Ph.D.** _____

Member **Joonghoon Park, Ph.D.** _____

Member **Su Cheong Yeom, Ph.D.** _____

Abstract

Exosomes are nanovesicles secreted from cells, which is important for the cell to cell communication. They are acting as shuttles to deliver biomolecules including proteins, lipids, mRNA, miRNA, and DNA between different cells. Exosomes offer significant pharmacological advantages including biocompatibility, stability, and low immunogenicity. However, translation to clinical applications is limited by low yield of production, heterogeneity, labor-intensive preparation procedure, and therapeutic loading. Cell-derived vesicles (CDVs) can be considered as artificial alternatives due to high productivity and biochemical compatibility to natural exosomes, which increase the clinical applicability of CDVs.

In this study, the therapeutic effects of CDVs through the delivery of pharmaceutical ingredients were evaluated, in particular for the recovery of myogenic potential and glucose metabolism in muscle cells. To this end, a proof-of-concept study was carried out by evaluating the delivery of green fluorescent protein (GFP) to the target cells by CDVs.

GFP-enriched CDVs (GFP^{Tg} CDVs) were generated from human embryonic kidney 293T (HEK293T) cells by micro-pore extrusions and OptiPrep density gradient ultracentrifugation. Out of 10^7 cells, 100 μg of GFP^{Tg} CDVs were generated, with 173.1nm in diameter, which was similar to the natural exosomes. Western blot revealed that GFP^{Tg} CDVs had exosomal marker CD9 and CD81. Furthermore, GFP protein and mRNA in GFP^{Tg} CDVs

were successfully detected in wildtype HEK293T cells from 60 min after treatment and in the cells for up to 48 hrs.

Based on these findings, pharmacological studies were conducted to determine whether the delivery of PROKR1 using CDVs can recover the differentiation ability of C2C12$^{Prokr1-/-}$ cells that lost myogenic potential. Based on these findings on target protein delivery through CDVs, researches turned to Prokineticin receptor 1 (*Prokr1*). *Prokr1* is important for the metabolic homeostasis in the skeletal muscle, and C2C12$^{Prokr1-/-}$ myoblasts differentiate into myotubes. *PROKR1*^{Tg} CDVs were generated from *PROKR1* overexpressing HEK293T cells, which had a diameter of 161.7nm, as well as the canonical exosomal marker proteins including CD9 and CD81. In addition, PROKR1^{Tg} CDVs had PROKR1 protein, and PROKR1 protein was successfully delivered to C2C12$^{Prokr1-/-}$ myoblast cells. The effect of the *PROKR1*^{Tg} CDVs on myoblast survival was determined by MTT assay, it was determined that the optimal concentration of the *PROKR1*^{Tg} CDVs for treatment was 25 μg/mL and below without cytotoxicity. The anti-apoptotic effect of *PROKR1*^{Tg} CDVs in myocytes was confirmed by flow cytometry analysis, and it revealed that *PROKR1*^{Tg} CDVs significantly reduced the apoptotic cell death of C2C12$^{Prokr1-/-}$ myocytes apoptotic cells by 8.4% compared to wild-type C2C12 myocytes. *PROKR1*^{Tg} CDVs enabled the myotube formation from C2C12$^{Prokr1-/-}$ myoblasts with authentic markers expression including up-regulation of *Myh7*, *Mb*, and *Myog*, and down-regulation of *Pax3*, *Pax7*, and *MyoD*. Furthermore, PROKR1^{Tg} CDVs-induced

C2C12$^{Prokr1-/-}$ myotubes showed insulin-stimulated glucose uptake, response comparable to the wile type C2C12 myotubes. These results imply that *PROKR1*^{Tg} CDVs could efficiently deliver *PROKR1* into C2C12$^{Prokr1-/-}$ myoblasts and recover their myogenic function.

Taken together, these results provide a basis for further evaluation of the therapeutic potential of *PROKR1*^{Tg} CDVs as therapeutic agents. CDVs appear to be an effective means of delivery active pharmaceutical ingredients and could be used for alternative therapy.

Keywords: apoptosis, C2C12, CDVs, GFP, glucose uptake, myogenesis, PROKR1

Student number: 2018-23506

Contents

List of Tables

List of Figures

List of Abbreviations

Akt/PKB	Protein kinase B
ASCs	Adipose-derived Stem Cells
ATCC	American type culture collection
BBB	Blood-brain barrier
BCA	Bicinchoninic acid protein assay
bEND.3	Brain-derived Endothelial cells.3.
cAMP	Cyclic AMP
CAMs	Cell adhesion molecules
CDVs	Cell-derived vesicles
CDK4	Cyclin-dependent kinase 4
CM	Cardiomyocyte
CNS	Central nervous system
DCs	Dendritic cells
DMEM	Dulbecco's Modified Eagle's Medium
DPBS	Dulbecco's Phosphate-Buffered Saline
ECs	Endothelial Cells
eGFP	Enhanced Green Fluorescent Protein
EPDCs	Epicardial-derived progenitor cells
ESCART	Endosomal sorting complex required for transport
FACS	Fluorescent-Activated Cell Sorting
FBS	Fetal Bovine Serum

FFA	Free Fatty Acid
GFP	Green Florence Protein
Glut4	Glucose transporter type 4
hCMECD3	Human Cerebral Microvascular Endothelial Cell
HEK293T	Human embryonic kidney 293T
HPLC	High-performance liquid chromatography
HRP	Horseradish peroxidase
HSP	Heat Shock Protein
HUVECs	Human umbilical vein endothelial cells
IHC	Immunohistochemistry
ILVs	Intraluminal endosomal vesicles
IRS	Insulin-Receptor Substrate
LFA-1	Lymphocyte antigen-1
LLC	Lewis lung carcinoma
MAPK	Mitogen-activated protein kinase
MCF	Michigan Cancer Foundation
MHC-2	Major Histocompatibility Complex class 2
miRNA	microRNA
MSC	Mesenchymal stem cell
MTT	3-(4,5-dimethylthiazol-2-yl)-2,5-diphenyltetrazolium bromide
MVBs	Multivesicular bodies
NK	Natural killer Cells
NOS	NO synthase

nt	Nucleotide
PBS	Phosphate-buffered saline
PCR	Polymerase chain reaction kit
PK2	Prokineticin 2
PI	Propidium iodide
PI3K	Phosphoinositide 3-Kinase
Prokr1	Prokineticin receptor 1
Prokr2	Prokineticin receptor 2
RME	Receptor-mediated endocytosis
RT-PCR	Reverse transcription polymerase chain reaction
SD	Standard deviation
SEC	Size exclusive chromatography
SKOV3	Ovarian cancer cell
SNAREs	Soluble N-ethylmaleimide-sensitive factor attachment protein receptors
Sphk-2	Sphingosine kinase 2
TEM	Transmission electron microscope
TGF-β1	Transforming growth factor beta 1
Tg	Transgenic
TSG-101	Tumor Susceptibility 101
t-SNAREs	target Soluble N-ethylmaleimide-sensitive factor attachment protein receptors
T2D	Type 2 Diabetes

VSMC	Vascular smooth muscle cells
v-SNAREs	Vesicle Soluble N-ethylmaleimide-sensitive factor attachment protein receptors
2-NBDG	2-(N-(7-nitrobenz-2-oxa-1,3-diazol-4-yl) amino)-2-deoxyglucose

Introduction

1. Exosomes

Exosomes are the smallest extracellular vesicles, with a diameter range from 30 to 150 nm [1-3], which is recognized important in cell to cell communication. Exosomes are released from multicellular organisms, exist extensively in various body fluids such as blood, urine, semen, lymph, milk, and saliva [4, 5]. Exosomes density ranges from 1.13 to 1.19 g/mL that can be separated by the sucrose gradient [6]. Exosomes have an endosomal origin, finally fuse with the cell surface and subsequently released from the cells. Exosomes are enveloped in a lipid bilayer membrane, reflecting they are originating from intracellular endocytic compartments. They acted as shuttles to deliver various biomolecules including proteins, lipids, mRNA, miRNA, and DNA between different cells (Figure 1). Exosomes express cell surface markers include tetraspanins (CD63, CD81, CD9), antigen presentation molecules (MHC I and MHC II) and others such as Alix, flotillin-1, Tsg101. Besides, the combination of markers is more reliable to define exosomes biochemically [7, 8]. Exosomes have been proposed for useful drug vectors than synthetic polymers because they are composed of cell membranes, and well tolerable to the cells [8].

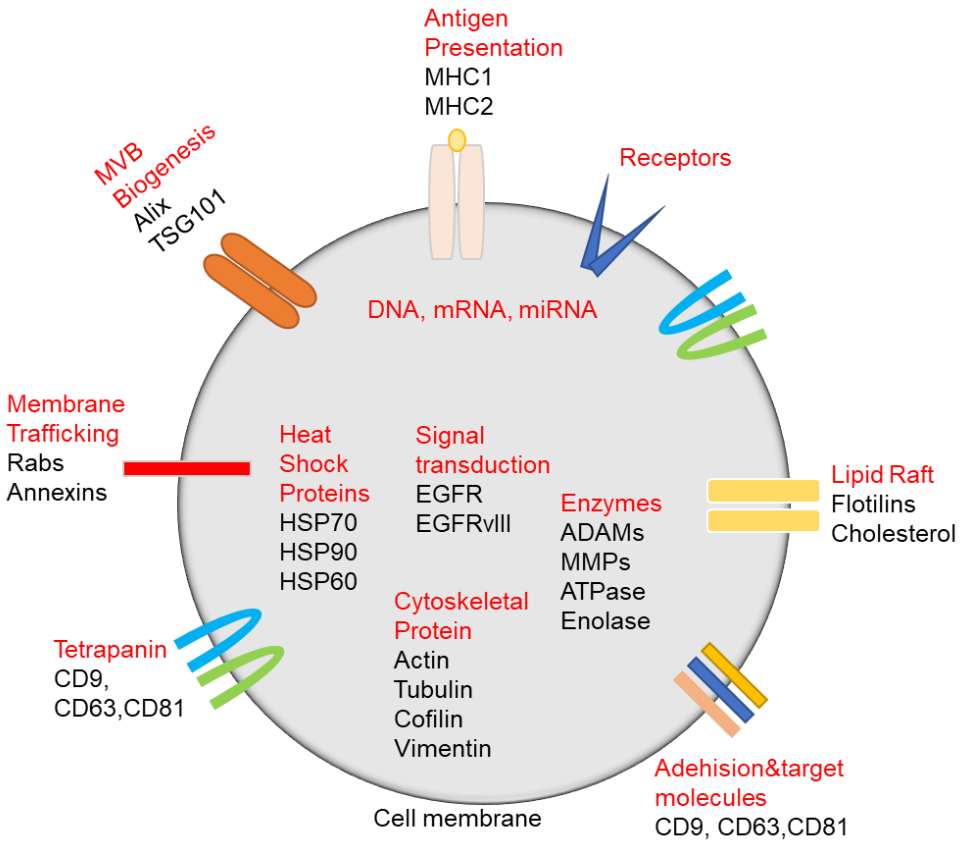

Figure 1. The molecular components of exosomes

Exosomes are known as a phospholipid bilayer enclosed vesicle containing various proteins on their surface membrane. Internally, exosomes are comprised of nucleic acids and numerous proteins. This image came from the report of Whitehead *et al*. (2017) [9].

1.1 Biogenesis

Most mammalian cells contain an endomembrane system and generate exosomes. Cell dynamic membrane compartments involve in the internalization of extracellular ligands or the organization of cellular components [10]. Portions of the plasma membrane are regularly internalized as endosomes, and early endosomes mature into late endosomes, which are called multivesicular bodies (MVBs) with intraluminal endosomal vesicles (ILVs) (Figure 2) [11] The ILVs become exosomes when the MVBs fuse with the cell surface in an exocytic manner [12, 13]. But another class of MVBs eventually delivered to lysosomes for degradation.

The sorting of protein complexes into MVB vesicles has at least two mechanisms, endosomal sorting complex required for transport (ESCRT)-dependent and ESCRT-independent mechanisms [14]. The ESCRT is a key mediator of MVB biogenesis. ESCRT complexes have several distinct ubiquitin-binding motifs [15, 16]. ESCRT-0 as a detection module for initiating the ESCRT pathway at endosomes. ESCRT-0 and ESCRT-I complexes recognize ubiquitinated proteins in the endosomal membrane. They are involved in MVB-dependent cargo sorting. ESCRT-II plays a critical role in initiating ESCRT-III complex formation [17], ESCRT-III complex is responsible for membrane budding [18]. Also, various cell types have different enrichment of ESCRT components and ubiquitinated proteins [19]. But lots of evidence favors another in ESCRT-independent pathway manner for sorting

exosomes cargo into MVB. Additionally, this pathway requires lipids such as ceramide which related to lateral phase separation and membrane invagination that may facilitate vesicle biogenesis [20]. Either the ESCRT-dependent or independent mechanism may act variously depending on the origin of the cell type.

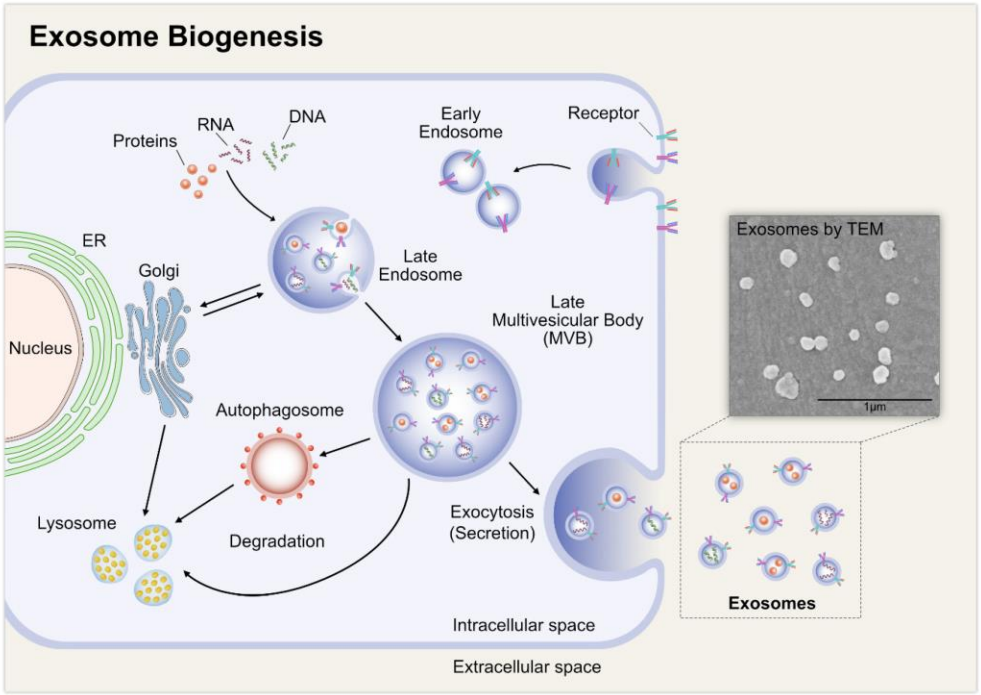

Figure 2. Exosomes biogenesis

Exosomes are generated in endosomes. Early endosomes develop into the late multivesicular body (MVB) harboring several exosomes. Exosomes contain various biomolecular such as proteins, RNA, and DNA. The representative image of exosomes is observed by the transmission electron microscope (TEM) in the right insert. This figure is cited from Gurunathan *et al*. (2019) [21].

1.2 Secretion

MVBs have two potential fates. One population of exosomes is delivered to lysosomes and degraded. Another population fuses with the plasma membrane and is released as exosomes because of the enrichment of cholesterol in the MVBs to facilitate the exosome secretion [22]. Some energy barriers must be overcome during this process. A lot of protein-lipid and protein-protein interactions have been shown to reduce these energy barriers and facilitate fusion as well as target-specific binding of exosomes.

Proteins implicated in membrane fusion include soluble N-ethylmaleimide-sensitive protein binding factor receptors (SNAREs), tethering factors, Rabs, and other Ras GTPases [23]. In human erythroleukemia cells, the secretion process involves the small GTPase Rab11[24]. It was shown that in T-cells, Rab27A and Rab27B play complementary roles in the spontaneous secretion of MHC class II-bearing exosomes [25]. Many Rabs proteins involved in exosome secretion especially Rab7 attached to the MVB recognizes receptor. Nonetheless, it is not known that various Rabs function at separate levels of exosomal secretion or are used differently used by particular types of cells [26]. The final step of exosome secretion needs the fusion of MVBs with the plasma membrane. This process possibly involves a specific combination of SNAREs, vesicular SNAREs (v-SNAREs) can interact with target SNAREs (t-SNAREs), to form a membrane-bridging SNARE complex, responsible for membrane fusion [27].

1.3 Uptake

Exosomes secreted from cells to extracellular space, carry functional proteins and nucleic acids to recipient cells, thus facilitate an impact on the cellular process of the recipient cells. To this end, exosomes must fuse with target cell membranes for endocytosis. Cells take up exosomes by a variety of endocytic pathways (Figure 3), including direct fusion, clathrin-dependent endocytosis, caveolin-mediated endocytosis, or clathrin/caveolin-independent endocytosis, phagocytosis, micropinocytosis, and lipid raft-mediated internalization [28]. Multiple receptor-mediated endocytosis (RME) has been linked to exosome internalization in each of these pathways. The recipient cell type may determine the specific type of internalization, each subtype of endocytosis has been defined in the exosomes and cell-derived mimetic vesicles internalization process. However, further work is required to establish the driving factors behind the specific mechanisms. Endocytosis mechanism depends on proteins and glycoproteins found on the surface of exosomes and the target cell, interestingly, exosomes entry into the same type of target cell via more than one route [29] (Table 1). For example, dendritic cells employ multiple endocytic pathways in the uptake of exosomes, including micropinocytosis, phagocytosis, and lipid raft mediated internalization[30] and receptor-mediated endocytosis [31]. Epithelial cells show the most diversity in exosome uptake of all the cell type, include clathrin-dependent endocytosis, caveolin-mediated endocytosis, lipid raft mediated internalization and multiple receptors [32, 33].

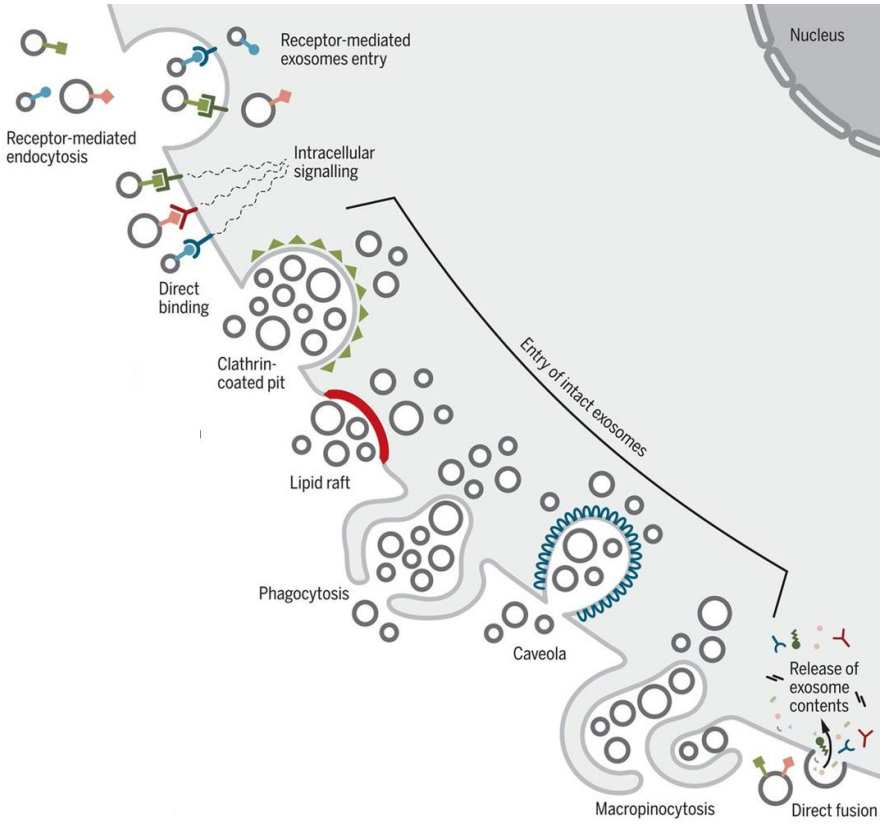

Figure 3. Cellular uptake of exosomes

The entry process of intact exosomes is divided by receptor-mediated endocytosis, clathrin-coated pits, lipid rafts, phagocytosis, caveolae, and micropinocytosis. The delivery of the exosomal content to the target cells is mediated by ligand-receptor-induced intracellular signaling or fusion to deposit the contents of the exosomes into the cytoplasm. This figure is modified from Kalluri *et al*. (2020) [34].

Table 1. Endocytosis pathways of exosomes and CDVs internalization

Endocytosis pathway	Recipient cell type	Recipient cell line	Cell source of exosomes	Reference
Phagocytosis	Epithelial	Ovarian cancer cell (SKOV3)	SKOV3	[35]
	DCs	Mouse primary	Mouse dendritic cell	[30]
Micropinocytosis	Epithelial	SKOV3	SKOV3	[35]
	Epithelial	Breast cancer (MCF7)	Normal breast epithelial cell (MCF-10A) cell-derived vesicles	[36]
Clathrin-mediated endocytosis	Endothelial	Brain microvascular endothelial	HEK 293T	[37]
	Epithelial	Breast cancer (MCF7)	Normal breast epithelial cell (MCF-10A) cell-derived vesicles	[36]
	Epithelial	SKOV3	SKOV3	[35]

(*Cont'd*) Table 1. Endocytosis pathways of exosomes and CDVs internalization

Endocytosis pathway	Recipient cell type	Recipient cell line	Cell source of exosomes	Reference
Caveolin-dependent endocytosis	Epithelial	Breast cancer (MCF7)	Normal breast epithelial cell (MCF-10A) cell-derived vesicles	[36]
	Endothelial	hCMECD3	Macrophage (RAW264.7)	[38]
	Endothelial	Brain microvascular endothelial	Embryonic kidney cell (HEK 293T)	[37]
Lipid raft-dependent endocytosis	Dendritic cell	Mouse primary	Mouse dendritic cell	[30]
	Epithelial	SKOV3	SKOV3	[35]
	Endothelial	Brain microvascular endothelial	HEK 293T	[37]

SKOV3: Ovarian cancer cell; DCs: Dendritic cells; MCF: Michigan Cancer Foundation; HEK 293T: Human Embryonic Kidney 293T; hCMECD3: Human Cerebral Microvascular Endothelial Cell; RAW264.7; Mouse macrophage cell;

1.4 Function and application

1.4.1 Biomarkers of diseases

It is well known that exosomes can be found in various body fluids. Since the exosomes contain different composition of proteins, lipids, and miRNA under different pathophysiological conditions, exosomes can be a useful biomarker for detection of diseases. Tetraspanins such as CD9, CD63 and CD81 are membrane proteins that are present in exosomes originated from nearly most of the cell types. CD9 expression is reduced in metastatic tumors relative to primary tumors and is associated with poor prognosis of advanced cancers [39]. The expression of CD63 is down-regulated upon melanoma progression [40]. CD81 is overexpressed in breast cancer [41]. Tumor cells secrete ten times more vesicles than normal cells, and it is assumed that the secreted vesicles are the most efficient means of transferring tumor and metastatic information to both normal and tumor cells [42]. TSG101 is also a useful biomarker to estimate the number of exosomes in tumors [43].

Exosomal miRNA analysis reveals that a certain type of miRNA in exosomes collected from the blood of patients can be used as a biomarker of lung cancer diagnosis [44]. Exosomal miR-92a concentrations are potential serum biomarkers for brown fat activity in mice and humans [45]. So, miRNA opening the prospect of early disease detection using circulating exosomes as screening tools. Inspiringly, exosomal miR-21 has a strong potential to be used as a universal biomarker to identify cancers [46].

1.4.2 Drug delivery system

Exosomes offer a variety of advantages over conventional drug delivery systems, such as viral or synthetic nanoparticles. Virus-based drug delivery systems fuse the advantages of natural viruses, including their outstanding capacity to enter host cells and integrate their viral genomic content into the host genome. However, their potential for insertional mutagenesis or oncogenesis, high cost of production and risk of immunogenicity limit their clinical use. Synthetic nanoparticle-based drug delivery systems, such as cationic polyplexes and lipoplexes, are known to be less immunogenic and mutagenic, but cytotoxicity, immunogenicity and low transfection efficiencies in vivo are still major challenges to address.

Exosomes have excellent advantages over the previously introduced drug delivery systems, and exosomes draw wide attention in the field of drug and nucleic acid delivery (Figure 4). The main potential advantages are biodistribution and biocompatibility. They are membrane-permeable and efficient after systemic delivery, and can also cross the blood-brain barrier [47]. Exosomes isolated from brain endothelial bEND.3 cells were able to deliver the rhodamine-123 dye across the blood-brain barrier (BBB) via the cardinal vein of zebrafish [48]. Most importantly, exosomes have immune tolerability, even with repeat administration, exosomes act well in non-immunosuppressed mice [49]. Exosome can carry proteins, miRNAs, siRNAs and other therapeutic drugs because these cargoes are stable inside of exosomes. They have tough lipid bilayer, which can protect cargo from degradation while

keeping bioactivity [50]. In fact, when marked exosomes were inserted into the bloodstream, they were observed to be distributed to tissues across the body within minutes, this makes them one of the fastest delivery vehicles [51]. In addition, markers on the surface of the exosomes act as targeting subunits, allowing them to bind to targeted cell types for mediating the exchange information and signal transductions [52, 53]. Altered surface molecules on exosomes have been shown to inhibit circulation clearance, such as blocking the scavenger receptor class A family to limit liver clearance [53]. Moreover, the small size and slight negative charge of exosomes make it possible to avoid clearance through the reticuloendothelial system, which in effect decrease renal clearance [54]. The most common method for loading small-molecule drugs is mixing the drugs solution and with exosomes suspension and incubating them at 25-37℃ [55]. Loading small molecule drugs and siRNA using electroporation can achieve 15-30% efficiency [56].

Despite these potential advantages, exosomes still at a primitive stage. The only studies that have been completed in terms of clinical applications are exosomes from dendritic cells in cancer immunotherapy, with mixed results [57]. One case report that intravenous MSC exosomes to treat host-refractory disease come out apparent short-term success [58]. At present, fundamental unresolved issues of exosome manufacturing include batch-to-batch variation, purity, quality control [59]. Additional studies are needed to determine positive and limited health aspects of exosomes, research concerning exosomes open a new perspective in our understanding of inter-organ cross-talk.

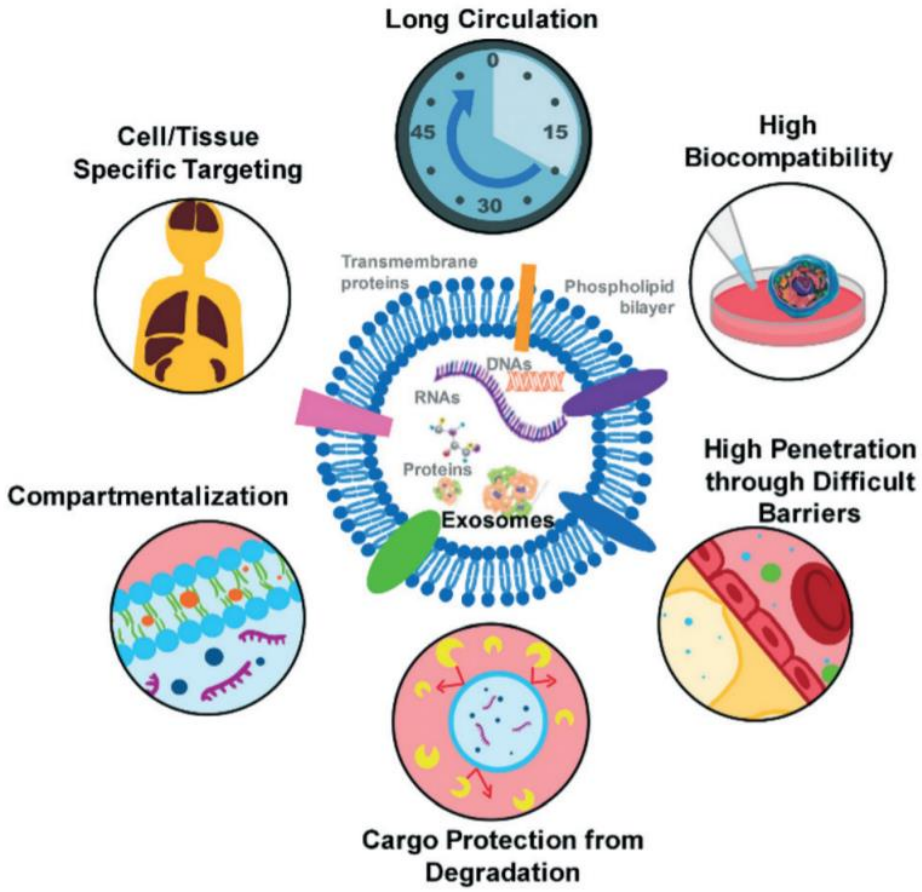

Figure 4. Advantages of exosomes

Exosomes carry DNAs, RNAs and protein, surrounded by tough lipid bilayer, which can protect exosomes from degradation. Because exosome originate from cell, they have high biocompatibility. Markers on the surface of the exosomes act as targeting subunits for target recipient cells. Exosome can be distributed to tissues though bloodstream within minutes. Small size and slight negative charge of exosomes decrease clearance in tissue. They are membrane-permeable and efficient after systemic delivery, and even can cross the blood-brain barrier. This figure is cited from Zhu *et al*. (2018) [60].

2. Cell-derived vesicles (CDVs)

CDVs are derived from cells and incorporate many cellular contents from the parental cells, such as membrane proteins, intracellular proteins, DNA, and RNAs. CDVs present many similarities with exosomes in aspects of their size, morphology, membrane proteins, and lipid composition [61]. Besides, RNA profiling revealed that CDVs enclose intracellular RNAs from parental cells, too.

2.1 General features of CDVs

Substantial evidence has shown the tendency of natural exosomes as drug delivery vehicles, they offer significant advantages including biocompatibility, stability and low immunogenicity. However, translation to clinical applications was limited by low yield, small scale manufacture, heterogeneity, labor-intensive isolation, and therapeutic loading. For these reasons, recent attention has been drawn to the possibility of generating cell-derived vesicles (CDVs) with high reproducibility, cost-effectiveness, scalable production and less immune response.

CDVs derived from cells with higher circulation retention and lower clearance rate, increased circulation time of their therapeutic cargo in the body, without the fear of any stimulated systemic toxicity than synthetic drug delivery systems. This robust and long-circulated endogenous nanocarriers shield the drug cargo from degradation and improve drug distribution to specific tissues[62]. The greater advantage of cellular vesicles is that they

escape from innate immune recognition, avoiding the rapid degradation and clearance by the immune defense systems[63].

2.2 Preparation of CDVs

Preparing CDVs are obtained artificially generated nanovesicles from broken cells. For example, scientists generate CDVs from hepatocyte cells by serial extrusions through filters and isolated these vesicles using an OptiPrep density gradient, these CDVs have 100-fold increased vesicle production yield [64]. It has been shown that nanovesicles express lymphocyte antigen-1 (LFA-1) that can bind with endothelial cell adhesion molecules (CAMs), overexpressed in tumors. Remarkably, drug-loaded CDVs into mice resulted in their decrease in tumor tissue size and subsequent reduction of tumor growth, while injecting free drug CDVs, there is no toxic side effects present [65]. Yoon *et al.* [66] had proposed an alternative method for generating CDVs. Living cells were sliced with microfabricated micro fabricated 500 nm-thick silicon nitride blades while flowing through a standardized microfluidic system (Figure 5). After cells sliced out of the system, the plasma membrane spontaneously self-assembled into approximately 100 to 300 nm diameter spherical CDVs. These successful examples show the potential to generate large scale CDVs for drug delivery. The above-described methods generate a high yield of CDVs from living cells in a short time. Exosomes isolation methods usually require up to 4 days, whereas CDVs production can be completed in a single day. However, it is currently unknown whether these

CDVs also have the benefits of natural exosomes, including low immunogenicity and biocompatibility.

2.3 Pharmacological effects of CDVs on various diseases

Recent reports that CDVs as viable nanocarriers for drugs in the treatment of various diseases (Table 2). CDVs were demonstrated to successfully deliver doxorubicin to tumor tissues and significantly reduced tumor growth without the adverse effects [67]. In another report, researchers used cellular carriers in liver regeneration. Cellular vesicles were formed by repeated extrusions of primary hepatocytes and then injected intravenously in mice. It was seen that the CDVs supplied the protein content of the parental cells and that they successfully facilitated hepatocyte proliferation in vitro and liver regeneration in vivo [64]. Strategies inspired by this study could lead to the usage of cell-derived vesicles in drug delivery.

Table 2. Examples of CDVs nanocarriers in the treatment of various diseases.

Cell source of CDVs	Therapeutic ingredient	Recipient cell or tissue	Function	References
Hepatocyte	Sphk-2	Hepatocyte	Facilitate hepatocyte proliferation in vitro and liver regeneration in vivo	[64]
U937	doxorubicin	HeLa	Reduced tumor growth	[67]
MCF-10A	CDK4 siRNA	Xenograft mouse tumor	Anti-tumor effect	[36]
MSC	paclitaxel	breast cancer cell BALB/c tumor mice	Inhibition of cancer growth	[68]
NIH3T3	c-Myc siRNA	λ820 cells	Inhibition of cellular c-Myc, target diseases associated with c-Myc over-expression, including cancer.	[69]
U937 and Raw 264.7	doxorubicin, 5-FU, gemcitabine, carboplatin	TNFα-treated HUVECs and CT26 cells	Reduce tumor growth	[70]

U937: Human monocytes cells; Sphk-2: sphingosine kinase 2; CDK4: Cyclin-dependent kinase 4; λ820 cells: mouse lymphoma cells; NIH3T3: mouse embryonic fibroblast cells; HUVECs: Human umbilical vein endothelial cells; Raw 264.7: Murine mouse macrophages; CT26: musculus colon carcinoma;

(*Cont'd*) Table 2. Examples of CDVs nanocarriers in the treatment of various diseases.

Cell source of CDVs	Therapeutic ingredient	Recipient cell or tissue	Function	References
Raw 264.7	radiolabeling agent ^{99m}Tc-HMPAO	BALB/c mouse	Biodistribution of exosomes and artificial counterparts in vivo	[71]
D3	mOct3/4 and mNanog	NIH-3T3 fibroblast cells	Gene delivery	[61]
D3	No intention of specific compounds	murine skin fibroblasts	Enhanced cell proliferation for regenerative medicine	[72]
NK	caspase-8 and caspase-3	glioblastoma, breast carcinoma, anaplastic thyroid cancer and hepatic carcinoma cells and xenograft glioblastoma mouse	Induce the apoptosis of the cancer cells	[73]
MSC	Rluc	LLC tumors	inhibit proliferation of LLC cells in vitro and to inhibit progression of LLC tumor xenografts in vivo	[74]

99mTc-HMPAO, 99mTc-hexamethylpropyleneamineoxime; D3: Murine mouse embryonic stem cell line; NIH3T3: mouse embryonic fibroblast cells; NK: Natural killer Cells; LLC, Lewis lung carcinoma;

3. Prokineticin receptor 1 (*PROKR1*)

Skeletal muscle is a major organ in body energy metabolism, and up to 70% of energy is derived from free fatty acid (FFA) in resting muscle. Insulin promotes glucose uptake into the skeletal muscle [75]. Patients of Type 2 Diabetes (T2D) are characterized by an increase in plasma free fatty acids [76]. High concentration of FFA can directly impair insulin signaling called insulin resistance in skeletal muscle. Obesity has been a known risk factor for T2D[77]. Obesity becomes a major health problem, due to its increasing prevalence and mortality. Obesity can induce a big risk factor for cardiovascular disease, diabetes mellitus, musculoskeletal disorders and some cancers. Obesity results from an excess energy imbalance between calorie intake and consumption, coupled with other metabolic disorders such as insulin resistance. Metabolically important proteins known as 'adipokines' secreted from adipose tissue which play a major role in appetite and insulin resistance [78].

Recently, prokineticin as a newly identified group of adipokines, have high levels in obese human white adipose tissues [79]. Prokineticin-2 (PK2) is a hormone of angiogenesis and anorexia, which activate two similar G-protein-coupled receptors: Prokineticin receptor 1 (*Prokr1*) and Prokineticin receptor 2 (*Prokr2*). The peripheral injection of prokineticin-2 has been shown to reduce food intake and body weight in lean and obese mice at the levels of dorsal vagal complex via *Prokr1* [80]. PK2 binding affinity for *Prokr1* is significantly

greater than *Prokr2* [81]. It is involved in diverse effects in different organs or tissues (Figure 5).

3.1 *PROKR1* in adipose tissue

Prokr1 is the main receptor expressed by preadipocytes and adipocytes [82]. In *Prok1*-deficient (*Prokr*1$^{ad-/-}$) mice, abnormal accumulation of abdominal fat mass was observed, attributed to the expansion of white adipose tissue, which indicates that *Prokr1* can suppress preadipocyte proliferation and differentiation, controlling adipose tissue expansion [79].

Adipose tissues are highly vascularized and the adipose vasculature exhibits phenotypic and functional plasticity to balance the metabolic needs of adipocytes. Adipose angiogenesis plays a major role in modulating insulin sensitivity [83]. Also, endothelial-specific *Prokr1* knockout mice (*Prokr1*$^{ec-/-}$) display insulin tolerance in adipocytes with low levels of capillary formation [84].

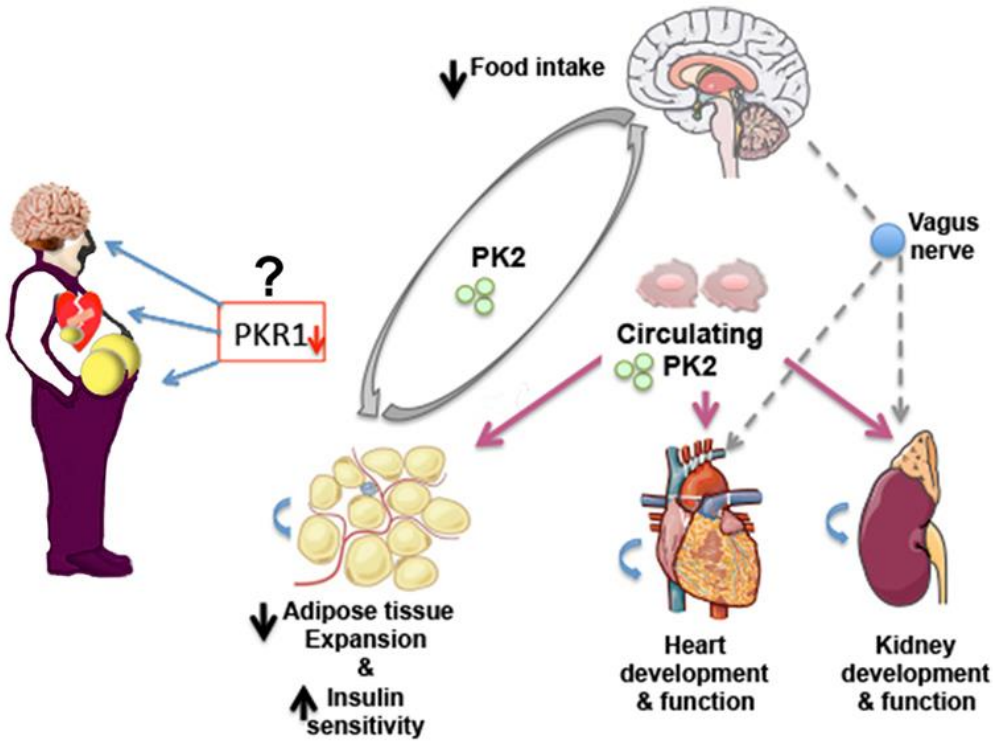

Figure 5. Prokineticin 2 (PK2)/PROKR1 signaling in different tissues

PK2/PROKR1 signaling may act as a new connector between the development of obesity, diabetes and cardiovascular diseases. *PROKR1* deficiency promotes WAT expansion and insulin resistance, and alters food intake in mice. Whether reduced level of *PROKR1* or functional mutated *PROKR1* involves these disorders in human needs to be studied. *PK2/ PROKR1* signaling in the CNS regulates food intake. *PK2* released from adipocytes controls preadipocyte conversion to adipocyte via *PROKR1* signaling and may affect food intake via CNS. Circulating or local *PK2* signaling via *PROKR1* contributes development and function of heart and kidney. *PKR1*: Prokineticin receptor 1; *PK2*: Prokineticin 2; CNS: central nervous system. This figure is cited from Nebigil *et al*. (2017) [85].

3.2 *PROKR1* in endothelial cells

Prokineticin-2 enhances endothelial cell proliferation and migration. Prokineticin receptors act selectively in endothelial cells (EC) derived from different tissues (Figure 6). *Prokr1* is strongly expressed in endothelial arteriole and vascular cells, while *Prokr2* is strongly expressed in fenestrated endothelial cells [86]. Prokineticin-2/*Prokr1* signaling promotes vessel-like formation in H5V cells by Akt and MAPK kinase-1 phosphorylation [87]. Two highly similar G protein-coupled receptors have divergent endothelial cell roles owing to their binding to two separate G signal proteins. Genetically induced *Prokr1* loss in the endothelial cells causes impaired capillary formation and trans-endothelial insulin delivery, leading to insulin resistance disorders [84]. Also, the loss of *Prokr1* in ECs leads to defective angiogenesis. Prokineticin-2 specifically facilitates angiogenesis by binding to *Prokr1*, through activating mitogen activated protein kinase (MAPK) and Akt pathway [88]. The endothelium plays a crucial function in the transcapillary transmission of insulin to the skeletal muscle interstitium, and this process is a speed-limiting stage in insulin-stimulated glucose uptake [89]. As a result, these data emphasize the role of *Prokr1* as a successful regulatory effects insulin delivery regulator and increases insulin sensitivity.

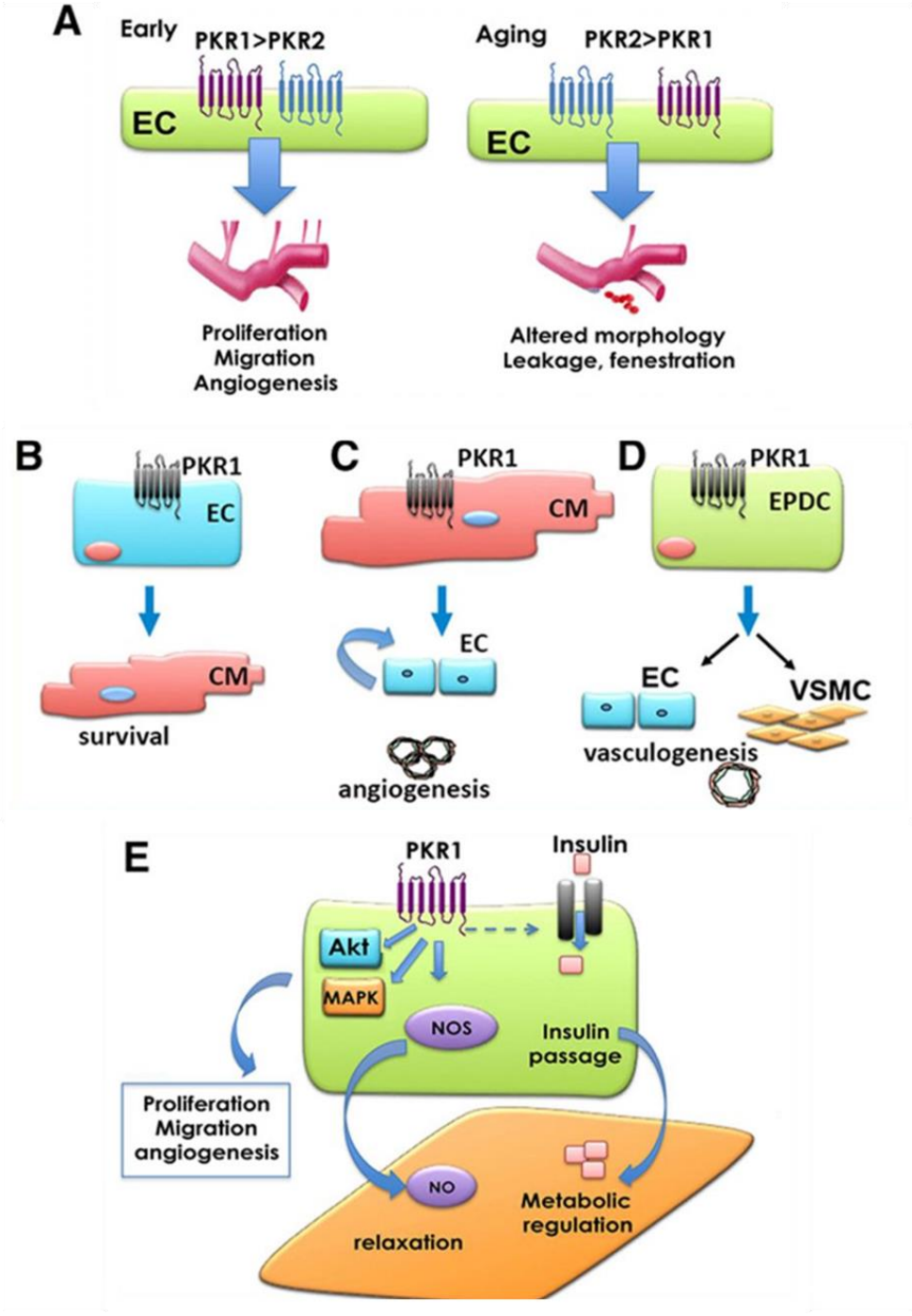
A
Early
PKR1>PKR2
EC
Proliferation
Migration
Angiogenesis
Aging
PKR2>PKR1
EC
Altered morphology
Leakage, fenestration
B
PKR1
EC
CM
survival
C
PKR1
CM
EC
angiogenesis
D
PKR1
EPDC
EC
VSMC
vasculogenesis
E
PKR1
Insulin
Akt
MAPK
NOS
Insulin
passage
Proliferation
Migration
angiogenesis
NO
relaxation
Metabolic
regulation

Figure 6. Functional effects of PROKR1 signaling transduction

A. The expression ratio of prokineticin receptor-1 (*PKR1*) to *PKR2* receptors in coronary endothelial cells (ECs). *PKR1* is more abundant in the early passages of coronary ECs. It mediates prokineticin-induced proliferation, migration, and angiogenesis. As they approach senescence, coronary ECs predominantly express *PKR2* with increasing passage number. *PKR2* mediates prokineticin-induced fenestration of ECs.

B. *PKR1*-mediated cellular interaction in heart. Endothelial *PKR1* signaling is a key signaling for cardiomyocyte (CM) survival.

C. CM *PKR1* signaling induces endothelial cell (EC) proliferation and angiogenesis.

D. EPDC *PKR1* signaling is important for differentiation of these cells into EC and smooth muscle cells to promote neovasculogenesis. VSMC: Vascular smooth muscle cells.

E. Role of *PKR1* on insulin transpassage in ECs. Activation or overexpression of *PKR1* in ECs increases insulin uptake. It also increases NO synthase (NOS) expression and phosphorylation, thereby regulating endothelial dependent relaxation. *PKR1* signaling via Akt and MAPK regulates proliferation, migration, and capillary formation. EPDC indicates epicardial derived progenitor cell; and MAPK, mitogen-activated protein kinases. This figure is cited from Nebigil *et al*. (2016) [90].

3.3 *PROKR1* in heart

Prokr1 plays a significant function in the cardiac progenitor cell particularly, *Prokr1* restores the pluripotency of the epicardial-derived progenitor cells (EPDCs) and triggers the differentiation into endothelial and vascular smooth muscle cells [88]. Transgenic *Prokr1* overexpressing mice in cardiomyocytes present postnatal coronary angiogenesis and vasculogenesis under paracrine regulation [91]. Interestingly, *Prokr1*null mice had contractile cardiomyocyte defects and apoptosis partially due to loss of *Prokr1* signaling in cardiomyocytes [92]. *Prokr1* signaling protects cardiomyocytes by activating the Akt signaling system against hypoxia-mediated apoptosis, transient expression of *Prokr1* lowers mortality and retains left ventricular activity by fostering angiogenesis contributes to cardiomyocyte survival or repair in the mouse model of myocardial infarction [93], it provides a novel therapeutic target to limit myocardial injury following ischemic events.

3.4 *PROKR1* in skeletal muscle

In a healthy human, glucose uptake in skeletal muscle is mediated by insulin, insulin promotes glucose uptake into the skeletal muscle in a dose-dependent manner. In insulin resistant states, insulin-stimulated glucose uptake in skeletal muscle is dramatically reduced through suppressing Akt pathway. The insulin signal pathway in the skeletal muscle involves the Insulin-Receptor Substrate (IRS)/Phosphoinositide 3-kinase (PI3K)/ protein kinase B (Akt) signal [94]. Firstly, insulin binds with the insulin receptor, activated insulin

receptor induces autophosphorylation on tyrosine residues. Then insulin receptor phosphorylates IRS-1 and IRS-2, which activate the PI3K/Akt pathway [95].

Tissue distribution analysis revealed that the expression of *Prokr1* was observed in skeletal muscle [82, 96]. *Prokr1* signaling has insulin-sensitizing effects on skeletal muscle [97]. There is evidence shows that *Prokr1* significantly activated PI3K/Akt signaling pathway in myotubes derived from C2C12. *Prokr1* activation enhanced insulin-stimulated Akt phosphorylation as well as Glut4 translocation to the plasma membrane and ameliorates insulin resistance in mouse skeletal muscle cells [98]. Taken together, *Prokr1* would be a potential target for the treatment of insulin resistance.

In this study, we investigate the *Prokr1* role in myogenesis and insulin resistance in skeletal muscle using murine myoblast cell line (C2C12). As exosome and can deliver protein and nucleic acid, here we test 1) if CDVs can deliver protein and RNA 2) whether PROKR1 membrane protein are taken up by C2C12$^{Prokr1-/-}$ cells and 3) whether PROKR1 protein can induce myogenesis and insulin-accumulated glucose uptake in C2C12$^{Prokr1-/-}$ cells.

Material and Method

1. Generation of genetically engineered cells

To establish the *PROKR1* transgenic human embryonic kidney 293T (HEK293T) cells, the genetic engineering express *PROKR1* vector was co-transfected with piggyBac transposon (Systems Biosciences, Palo Alto, CA, USA) using Lipofectamine 3000 (Invitrogen, Carlsbad, VA, USA) according to the manufacturer's protocol (Figure. 7). Seeding cells in culture plates until it reaches to 80% confluency. Wash cells with phosphate-buffered saline (PBS; Gibco, Grand Island, NY, USA) and refresh them with 2 ml of the culture medium with no antibiotic-antimycotic agent. In each well was added the plasmid DNA-lipid complex consisting of 7.5 μL Lipofectamine 3000 reagent in 250 μL Opti-MEM (Invitrogen, Carlsbad, VA, USA) and 10 μL P3000 reagent with a 2.5 μg piggyBac transgene vector and piggyBac transposase plasmid in 250 μL Opti MEM. One day after lipofection, 10 μg puromycin mL-1 was added to select the cells stably transfected with the transgene.

To knock out the *PROKR1* gene in HEK293T cell lines, the expression vector RNA (gRNA) guide and Cas9 carrying the enhanced green fluorescent protein (eGFP) transgene (Sigma-Aldrich, St. Louis, MO, USA) were co-transfected at a ratio of 1:1 (2.5 μg each) using Lipofectamine 3000. HEK293T cell lines were harvested and resuspended one day after lipofection in PBS containing 1% bovine serum albumin (BSA; Sigma, St. Louis, MO, USA), and passed through a 40 μm cell strainer (Becton, Dickinson and Company,

Franklin Lakes, NJ, USA) for fluorescence-activated cell sorting using a FACS Aria TM III cell sorter (Becton, Dickinson and Company). Single GFP-positive HEK293 T cell lines were picked under a microscope after enrichment of GFP-positive cells, and seeded on individual wells of a 96-well plate.

2. Cell culture

Wildtype HEK293T cells were purchased from American type culture collection (ATCC, Manassas, VA, USA). *GFP*^{Tg} HEK293T cells, *PROKR1*^{Tg} HEK293T cells and HEK293$^{PROKR1-/-}$ cells were produced by professor Taesub Park, they were cultured in 4.5 g/L D-glucose Dulbecco's Modified Eagle's Medium (DMEM; Gibco, Grand Island, NY, USA) which include 10% (v/v) exosome-free FBS, 1% (v/v) antibiotic-antimycotic (Gibco, Grand Island, NY, USA) at 37°C in 5% CO2/95% O2 humidified air. After cells confluency is ~80%, cells are ready for generate CDVs.

C2C12 cell line (ATCC) and C2C12$^{Prokr1-/-}$ cells were maintained in 1 g/L D-glucose DMEM (Gibco) that include 20% v/v exosome-free FBS, 1% (v/v) antibiotic-antimycotic (Gibco) and differentiated in 4.5 g/L DMEM with 2% (v/v) horse serum (Gibco) after reaching 80% confluence. The C2C12 myoblasts were differentiated into myotube after differentiation 6 days.

3. Preparation of CDVs

The adherent transgenic HEK293T cells were detached and resuspended in DPBS at 10^7 cells/ml. The cell suspension was serially extruded 7 times

through polycarbonate membranes filters with pore sizes of 10, 5 and 1 μm Nucleopore Trac-Etch Membrane (Whatman, Avanti Polar Lipids, Inc, Alabaster, Alabama, USA) using micro-extruder (Whatman, Avanti Polar Lipids) (Supplementary figure 1A). Unpurified CDVs was through 0.2 μm filter to exclude bigger size of CDVs. To perform two-step sucrose OptiPrep (Sigma, St. Louis, MO, USA) density gradient ultracentrifuge, 50% OptiPrep (1.5 ml), 10% OptiPrep (1.5 ml) and the sample (7 ml) were placed in an ultracentrifuge tube from bottom to top and then ultracentrifuge at 100,000×g for 2hr at 4℃. CDVs were obtained from the interface of 50% and 10% OptiPrep layers and then washed with DPBS. At last step, resuspend purified CDVs in DPBS.

4. Size distribution analysis of CDVs

The size distribution of CDVs was measured by Malvern Zetasizer Nano ZS (Malvern, Worcestershire, UK). CDVs (10ug) were diluted in 500ul DPBS, put in the disposable cuvette ZEN0040 (Malvern, Worcestershire, UK) and do measurement. Three independent sample were measured.

The CDVs purity is confirmed by 1260 Infinity high-performance liquid chromatography (HPLC; Agilent, Santa Clara, CA, USA). The size-exclusion column (SEC, CG103-25) is used for HPLC. HPLC system equipped with an autosampler and UV detector. Before SEC, prepare 100% methanol, 20% methanol and PBS solution. Make 20% methanol and PBS solution through 0.2 μm filter and sonicate 15 min to remove air. Importantly, be sure to remove

air from the pipe every time change the mobile phase. First, running 100% methanol overnight and change to PBS buffer (PH=7.4) for HPLC mobile phase. After the mobile phase is stable, 30 μL sample was injected, and the flow rate is 0.5ml/min. The column is calibrated with a high molecular weight kit (Gel filtration Calibration Kit HMW, GE Healthcare; Kenilworth, NJ, USA), which contains 6 proteins from 44 kD (ovalbumin) to 2000 kD (blue dextran). CDVs are detected at a UV wavelength of 254 nm.

5. Quantitative analysis of CDVs content

The quantities of CDVs were determined using the Bradford (Bio-Rad, Hercules, CA, USA) protein assay. The total protein of CDVs was measured using Bicinchoninic acid (BCA) protein assay kit (Thermo Fisher scientific, MA, USA). CDVs were lysed using a Radio-immune-precipitation assay (RIPA; Thermo scientific, MA, USA) buffer for 5 min and their lipids were removed by centrifugation at 10,000×g for 10 min. CDVs RNA were extracted by TRIzol Reagent (Ambion, Life Technologies, Austin, TX, USA) and chloroform. Finally, CDVs RNA was dissolved in RNase Free Water (Qiagen, Venlo, Nederland). To confirm GFP^{Tg} CDVs contain mRNA, extract GFP^{Tg} CDVs RNA. After extract sample RNA using TRIzol method, RNAs were qualified using a spectrophotometer (IMPLEN).

6. Western blotting

Cells and CDVs were lysed by Pierce RIPA buffer (Thermo Fisher Scientific). Lipid particles were removed at 14000×g for 15min, then protein concentration was determined by the BCA Protein Assay kit (Thermo Fisher Scientific). Equal amount of protein (30 μg) denatured at 95℃, 5min, then loaded into each well and running in 10% SDS-PAGE gel at 100 V for 80 min. Proteins were transferred to nitrocellulose membranes and run at 100 V for 2 hrs. Check the transfer quality using Ponceau S solution (Sigma, St. Louis, MO, USA) staining. Then nitrocellulose membranes were blocked in 5% BSA (Sigma, St. Louis, MO, USA) in TBST (0.2% tween20 in TBS), then incubated overnight at 4℃ with primary antibody. The samples were coated with secondary antibody for 1 h at room temperature, and then proteins were detected by an enhanced chemiluminescence kit (Bio Rad). The primary antibodies were anti-β-Actin (Santa Cruz, sc-47778), anti-CD9 (Abcam, ab92726), anti-CD81 (Abcam, ab109201), anti-Prokr1 (Biorbyt, orb162427); the secondary antibodies were anti-mouse HRP (Thermo Fisher, 31460), anti-rabbit HRP (Thermo Fisher, 31430). Primary antibody anti-Prokr1was diluted 1:500, anti-β-Actin and CD81 were diluted 1:1000, anti-CD9 was diluted 1:2000. The secondary antibody was diluted 1:1000.

7. RT-PCR

To confirm *GFP*^{Tg} CDVs maintained in wildtype cells, we treat 200 μg/ml *GFP*^{Tg} CDVs to wildtype HEK293T cells in 48 well plate, and harvest

wildtype HEK293T cells at different time point using 0.25% trypsin-EDTA (Gibco，Grand Island, NY, USA). Samples of RNAs (<5 μg) were reverse-transcribed using a reverse transcription kit (Invitrogen, Carlsbad, CA, USA) at 65℃ for 5 min, at 50℃ for 60 min, at 70℃ for 15 min and 37℃ for 20 min serially. Polymerase chain reaction kit (PCR) was performed using a PCR kit (Invitrogen, Carlsbad, CA, USA) with primers for human-*GAPDH* and *GFP*. The PCR process consisted of denaturation at 95℃ for 4 min, followed by 32cyclcles of amplification at 95℃ for 30 s, 60℃ for 30 s, 72℃ for 1 min and extension at 71℃ for 5 min.

Quantitative PCR was performed using Step One Plus Real-Time PCR System and Power SYBR Green PCR Mater Mix (Applied Biosystems, Foster City, CA, USA). The process consisted of an initiation step at 95℃ for 10 min, and then 40 cycles of amplification at 95℃ (denature) for 15 s, 60℃ (anneal/extend) for 1 min, and melting curve analysis. Data analysis were performed by using ΔΔCt method, using *Gapdh* as control gene for quantification. Primers were listed in table 3.

Table 3. Primers used in this study

Gene symbol	Forward	Reverse	Tm (℃)	Amplicon (bp)
Gapdh	AGGTCGGTGTGAACGGATTTG	TGTAGACCATGTAGTTGAGGTCA	60	123
h-GAPDH	AGGGCTGCTTTTAACTCTGGT	CCCCACTTGATTTTGGAGGGA	60	206
Prokr1	GCTCTGGTTCGCAGGTTGAA	GCAAGGTTGACGACTCCTCT	60	119
h-PROKR1	CAATTCCAGGACGTTCTTTGCT	GCAGTTTCTTGTAGCGGACCA	60	122
GFP	CCGCATCGAGAAGTACGAGG	CTGCGGATGATCTTGTCGGT	60	147
Myh7	ACTGTCAACACTAAGAGGGTCA	TTGGATGATTTGATCTTCCAGGG	60	114
Myoglobin	CTGTTTAAGACTCACCCTGAGAC	GGTGCAACCATGCTTCTTCA	60	108
Myogenin	GAGACATCCCCCTATTTCTACCA	GCTCAGTCCGCTCATAGCC	60	106
Pax3	TTTCACCTCAGGTAATGGGACT	GAACGTCCAAGGCTTACTTTGT	60	275
Pax7	TCTCCAAGATTCTGTGCCGAT	CGGGGTTCTCTCTCTTATACTCC	60	132
MyoD	CTACAGTGGCGACTCAGA	GTAGTAGGCGGTGTCGTA	60	118

8. Cell uptake analysis of CDVs

Using the Dako pen to write a circle on the glass slide, then coat with poly-L-Lysine (Sigma, St. Louis, MO, USA) on surface within the circle. Rock glass slide gently to ensure evenly coating. After 5 min, remove poly-L-Lysine solution and rinse slide surface with ultrapure distilled water (Life Technology). After 2 hrs of drying the glass slide on clean bench, seed condensed *GFP*^{Tg} CDVs in DPBS. Wait for at least 2 hrs until CDVs attach to the slide in 37°C humidified cell incubator. Adding 10% formalin solution for 10 min, then replace it with DPBS. Using nail polish solution fix the coverslip border. After drying 30min, detect Green Florence protein by Cytation 5 (BioTek, Canada). Fresh *PROKR1*^{Tg} CDVs were applied to wildtype HEK293T cells for 24 hrs at 100 μg/ml in 96 well plate, real-time uptake process under Bright and GFP channel were observed under Cytation Cell Imaging Multi-Mode Reader of Cytation 5. The reader saves one picture every 20 min automatically.

9. Cell viability assay

To detect *PROKR1*^{Tg} CDVs toxicity dose range to C2C12$^{Prokr1-/-}$ myoblast cells, cell proliferation MTT assay (Invitrogen, Carlsbad, CA, USA) is measured. C2C12$^{Prokr1-/-}$ cells (1×10^4 cells/each well) were seeded in 48 well plate until cells attach to the bottom of plate. *PROKR1*^{Tg} CDVs was applied to C2C12$^{Prokr1-/-}$ myoblast cells for 48 hrs and change growth medium every 24 hrs. As the presence of phenol red in the MTT assay can affect results, no phenol red DMEM is used. Cells were incubated with 20 μL of 12 mM MTT

stock solution at 37℃ for 4 hrs, then add 200 μL of SDS-HCl solution to each well and mix thoroughly. After 4 hrs, read absorbance at 570 nm.

10. Flow cytometry analysis

C2C12$^{Prokr1-/-}$ cells (2×10^4 cells/each well) were incubated in 6 well plate until cells attach to the bottom of plate. *PROKR1*^{Tg} CDVs were treated to C2C12$^{Prokr1-/-}$ myoblast cells at 25 μg/ml for 3 days with daily change medium, then change to the differentiation medium without CDV treatment. Cell apoptosis was evaluated at differentiation day 3 using Alexa Fluor 488 annexin V cell Apoptosis Kit (Thermo Fisher Scientific, Waltham, MA, USA) with Alexa Fluor 488 annexin V and PI for Flow Cytometry (Invitrogen, Carlsbad, CA, USA). Analyze the stained cells by flow cytometry, measuring the fluorescence emission at 521 nm and 617 nm. Apoptotic cells were counted in 3 dependent samples and calculated early and late apoptotic cells.

11. Actin staining

C2C12 cells were seeded on chamber slide (Thermo Fisher Scientific, Waltham, MA, USA) at a density of 1×10^4 cells/slide in growth medium. After 3 days of CDVs treatment and 6 days of differentiation, cells were fixed in 10% Neutral buffered formalin (Sigma, St. Louis, MO, USA) for 10 min, and then washed with DPBS 3 times. Fixed cells were permeabilized with 0.1% (v/v) Triton X-100 for 10 min, and blocked with 2% (v/v) BSA in DPBS for 60 min at room temperature. Cells were then stained with Alexa Fluor® 488 phalloidin (Thermo Fisher Scientific, Waltham, MA, USA) for 60 min. Then wash with

DPBS three times, remove slide upper structure, cells were incubated with Antifade Mounting Medium with DAPI (Maravai Life Sciences, San Diego, CA, USA), then overnight in the dark at room temperature. Cells were observed with a fluorescence microscope and then stored in the dark at -4°C.

12. Glucose uptake assay

Glucose uptake activity was measured using 2-[N-(7-nitrobenzene-2-oxa-1,3-diazol-4-yl) amino]-2-deoxy-D glucose (2-NBDG) (Thermo Fisher Scientific, Waltham, MA, USA), a fluorescent D-glucose analog. Firstly, differentiated muscle cells on 24-well plates were treated with no glucose DMEM 2 hr, myotubes were incubated with or without 100 nM insulin (Cell applications, Inc, San Diego, CA, USA) for 30 min. Next, myotubes were transferred to fresh no glucose DMEM medium supplemented with 80 μM of 2-NBDG for 30 min. After cold DPBS three times wash, the fluorescence intensity of cellular 2-NBDG in each well was measured at excitation/emission wavelength of 485/535 nm using Cytation 5, Multi-Mode Reader (BioTek).

13. Statistical analyses

Statistics analyses were performed using GraphPad Prism 8 software. All results were expressed in mean ± standard deviation (SD). *P*-value was calculated using two-sided Student's t-test, and p-value < 0.05 was considered significant.

Result

1. Generation of genetically engineered cells

PROKR1 overexpressed cells (*PROKR1*^{Tg} HEK293T) were generated by using piggyBac vector in HEK293T cells (Figure 7A). *PROKR1/Prokr1* knock-out cells were prepared by using CRISPR/Cas9 method. To generated *PROKR1*-deficient HEK293T cells (*PROKR1*$^{-/-}$ HEK293T), a pair of gRNA was used to target the 2nd exon of *PROKR1* genes, and it resulted in 151 bp deletion (Figure 7B). To produce *Prokr1*-deficient C2C12 cells (*Prokr1*$^{-/-}$ C2C12), another pair of gRNA was used to target the 2nd exon of *Prokr1* genes, which produced 24 bp- and 128 bp- deleted homozygous cells (Figure 7C). All of the *PROKR1/Prokr1*-engineered cells were subjected to FACS based on GFP signal and clonal proliferation of the sorted single cell. RT-PCR showed that *PROKR1* mRNA was significantly up-regulated in *PROKR1*^{Tg} HEK293T cells ($p < 0.001$). In mock control and *PROKR1*$^{-/-}$ HEK293T cells, basal levels of *PROKR1* mRNA expression was observed, and it was supposed to be from truncated mRNA (Figure 7D). Protein levels of PROKR1/Prokr1 were significantly up-regulated in PROKR1Tg HEK293T cells and wild type (WT) C2C12 cells, and there was no detectable expression of PROKR1/Prokr1 protein in WT HEK293T cells, *PROKR1*$^{-/-}$ HEK293T cells, and *Prokr1*$^{-/-}$ C2C12 cells (Figure 7E-F). These results demonstrated that *PROKR1/Prokr1* overexpression or knock-out cells were well prepared and they were used as CDV donor cells as well as CDV subject cells in the subsequent experiments.

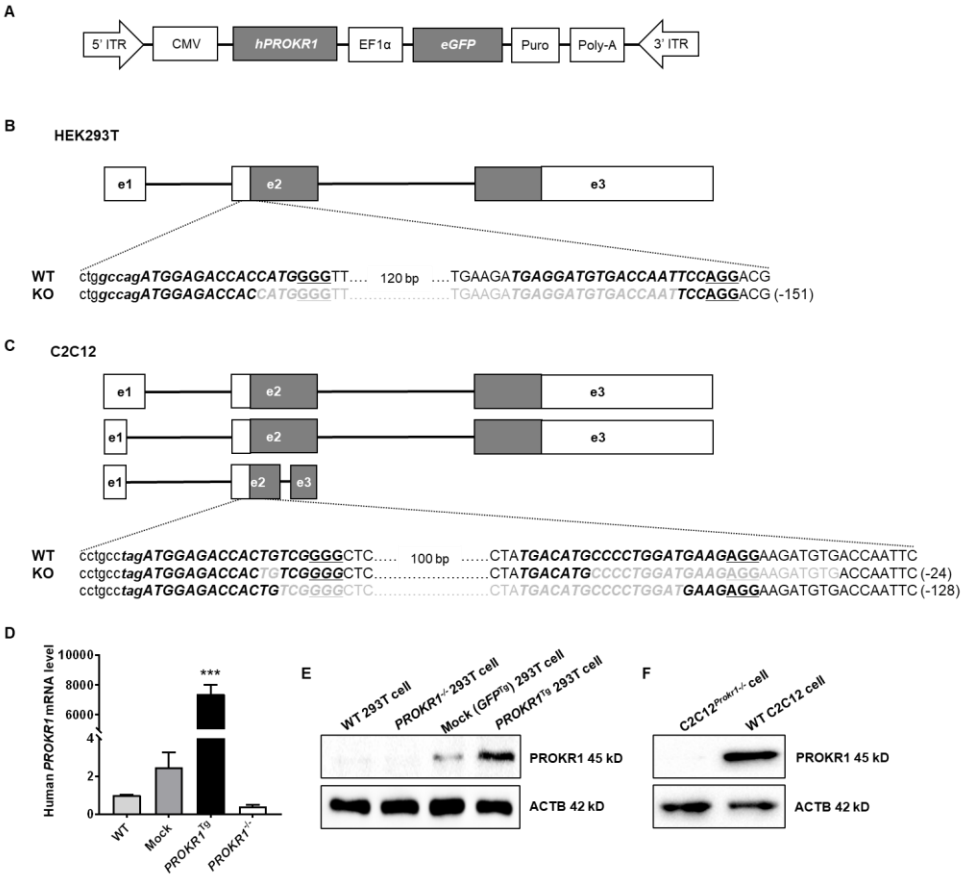
A
5' ITR
CMV
hPROKR1
EF1α
eGFP
Puro
Poly-A
3' ITR
B
HEK293T
e1
e2
e3
WT ctggccagATGGAGACCACCATGGGGTT.... 120 bp ....TGAAGATGAGGATGTGACCAATTCCAGGACG
KO ctggccagATGGAGACCACCATGGGGTT.....TGAAGATGAGGATGTGACCAATTCCAGGACG (-151)
C
C2C12
e1
e2
e3
WT cctgcctagATGGAGACCACTGTCGGGGCTC..... 100 bp .....CTATGACATGCCCCTGGATGAAGAGGAAGATGTGACCAATTC
KO cctgcctagATGGAGACCACTGTCGGGGCTC.....CTATGACATG.....ACCAATTC (-24)
cctgcctagATGGAGACCACTGTCGGGGCTC.....CTATGACATGCCCCTGGATGAAGAGGAAGATGTGACCAATTC (-128)
D
Human PROKR1 mRNA level
10000
8000
6000
4
2
0
***
WT
Mock
PROKR1tg
PROKR1-/-
E
WT 293T cell
PROKR1-/- 293T cell
Mock (GFPtg) 293T cell
PROKR1tg 293T cell
PROKR1 45 kD
ACTB 42 kD
F
C2C12Prokr1-/- cell
WT C2C12 cell
PROKR1 45 kD
ACTB 42 kD

Figure 7. Generation of *PROKR1/Prokr1* engineered cells

A. PiggyBac expression vector construct for human P*ROKR1* gene.

B-C. CRISPR/Cas9-mediated *PROKR1/Prokr1* deletion in HEK293T cells and C2C12 cells. Upper characters indicate coding region. Italic characters indicate gRNA binding sites. Underlined characters indicate PAM sequences. Gray characters indicate the deleted sequence in KO cells. The length of deleted sequences is depicted in parenthesis. e = exon.

D. RT-PCR analysis mRNA expression of *PROKR1*. Mock: PiggyBac vector without *PROKR1*. Bars indicate mean ± SD, N = 3, ***$p < 0.001$ vs. WT, Dunnett's multiple comparison test.

E-F. Western blot analysis of PROKR1/Prokr1 in HEK293T cells and C2C12 cells. ACTB is used as an internal control.

2. Generation and Characterization of CDVs

To exploit the beneficial effect of CDVs, a more efficient CDVs generating system must be created. The process of the preparation of CDVs from HEK293T cells is illustrated in Figure 8A. After extruding cells through serial polycarbonate membranes, CDVs were purified by two-step OptiPrep density gradient. And to confirm if the OptiPrep density gradient is effective, CDVs comes from before and after density gradient step was performed to Size-Exclusion Chromatography (SEC). CDVs of before density gradient step come out several peaks, while CDVs of after density gradient step only have one peak, the peak with a retention time of 3.2 min stands for the purified CDVs while the rest peaks are impurities of small size (Figure 8B). The results revealed OptiPrep density gradient is a useful way to get purified CDVs.

CDVs isolated from transgenic (Tg) HEK293T cells were characterized by size, surface markers, particle yield, and protein and RNA amount. The total CDVs size distribution is compared among four types of CDVs. The *GFP*^{Tg} CDVs mean diameter is 173.1±12.0 nm, 168.1±10.2 nm in wildtype CDVs (Figure 9A), 161.7±12.3 nm in *PROKR1*^{Tg} CDVs, and 152.6±2.9 nm in *PROKR1*$^{-/-}$ CDVs (Figure 9B). Four types of CDVs show that the mean diameter is around 160nm. According to the western blotting result, four types of CDVs show positive exosome markers expression, including CD9 and CD81, and *PROKR1*^{Tg} cells and CDVs have PROKR1 protein expression (Figure 9C). CDVs generate from 10^7 cells were indirectly quantified by

measuring membrane protein using Bradford. Additionally, *PROKR1*^{Tg} CDVs and *GFP*^{Tg} CDVs yield significantly increase by 40.8% and 43.7% respectively ($p < 0.01$) more than wildtype CDVs, and *PROKR1*$^{-/-}$ CDVs yield have no significant differences with wildtype CDVs (Figure 9D), while CDVs yield is more than natural exosome. *GFP*^{Tg} CDVs and *PROKR1*^{Tg} CDVs protein amount significantly increases by 65.8% and 90.5% respectively ($p < 0.01$) more than wildtype CDVs. RNA amount generated from 10^7 cells also be measured. *GFP*^{Tg} CDVs and *PROKR1*$^{-/-}$ CDVs RNA amount significantly increase by 138.3% and 98.8% respectively ($p < 0.001$) more than wildtype CDVs. The RNA amount of *PROKR1*^{Tg} CDVs more 149.7% ($p < 0.01$) than wildtype CDVs. To identify RNA quality in the CDVs, bioanalyzer was conducted. Various RNAs contain rRNA, tRNA and microRNA were detected in *GFP*^{Tg} CDVs (Figure 8C). 18S RNA and 28S RNA height ratio in RNA profile are around 1:2. Also, the electrophoresis results indicate that high quality-mRNA was successfully encapsulated into the *GFP*^{Tg} CDVs.

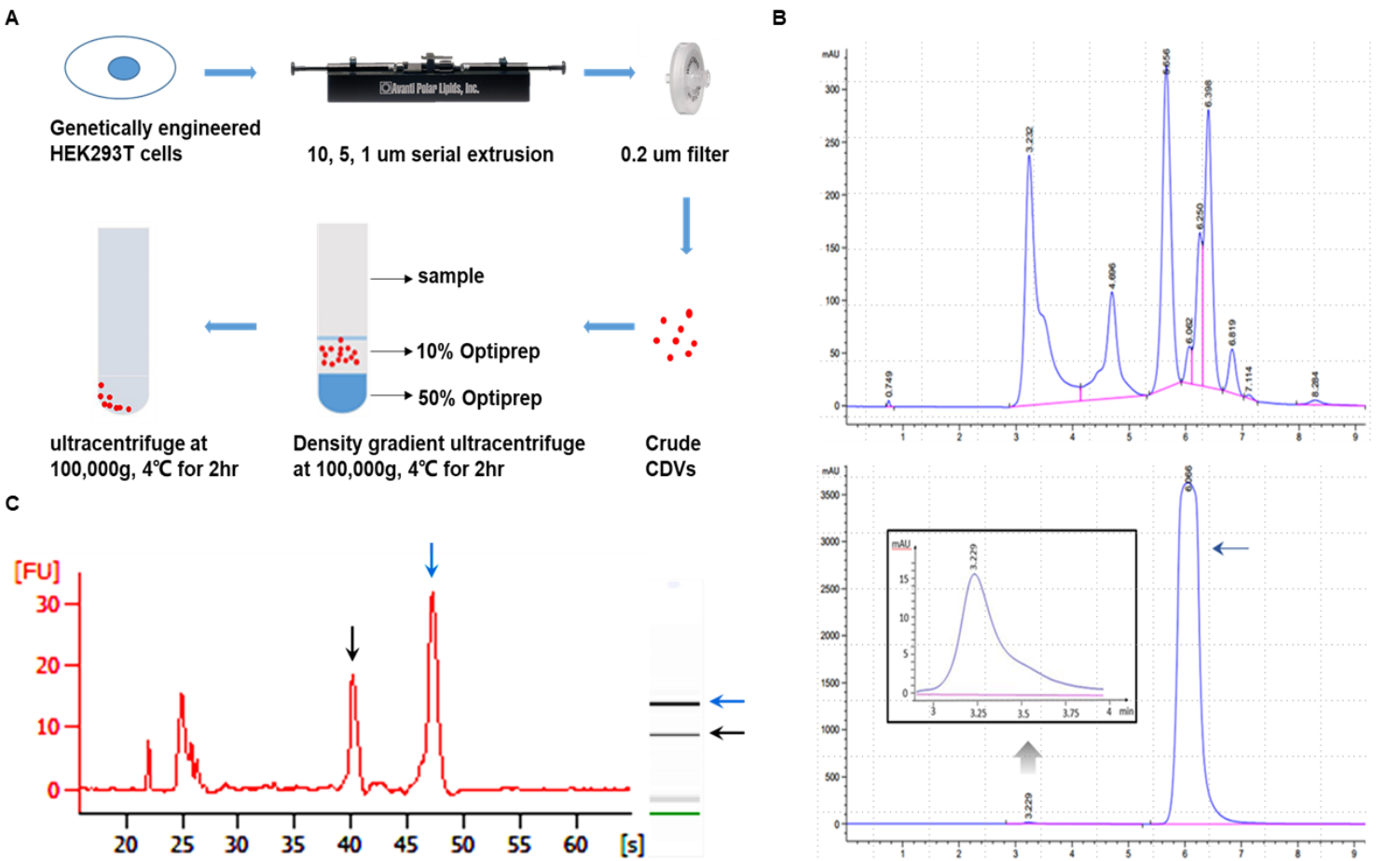
A
Genetically engineered HEK293T cells
10, 5, 1 um serial extrusion
0.2 um filter
sample
10% Optiprep
50% Optiprep
ultracentrifuge at 100,000g, 4℃ for 2hr
Density gradient ultracentrifuge at 100,000g, 4℃ for 2hr
Crude CDVs
B
C
[FU]
[s]

Figure 8. Production of CDVs generate from genetically engineered HEK293T cells

A. Schematic diagram of production and purification of CDVs from cells. OptiPrep: density gradient medium containing iodixanol. The red dots represent the CDVs.

B. Particle size analysis of CDVs by size-exclusion chromatogram (SEC). Top panel: chromatogram of *GFP*^{Tg} CDVs before OptiPrep density gradient purification. Bottom panel: chromatogram of *GFP*^{Tg} CDVs after OptiPrep density gradient purification. Insert shows magnified chromatogram at 3.2 min. Horizontal axis represents retention time (min), and vertical axis represents the florescence (FU). Blue arrow: OptiPrep, gray arrow: purified *GFP*^{Tg} CDVs.

C. RNA profile in *GFP*^{Tg} CDVs. Left panel: chromatogram of different RNA types of RNAs. Horizontal axis represents retention time (s), and vertical axis represents the CDVs particle fluorescence unit (FU). Right panel: electrophoresis of different type of RNAs. Black arrow: 18s rRNA; blue arrow: 28s rRNA.

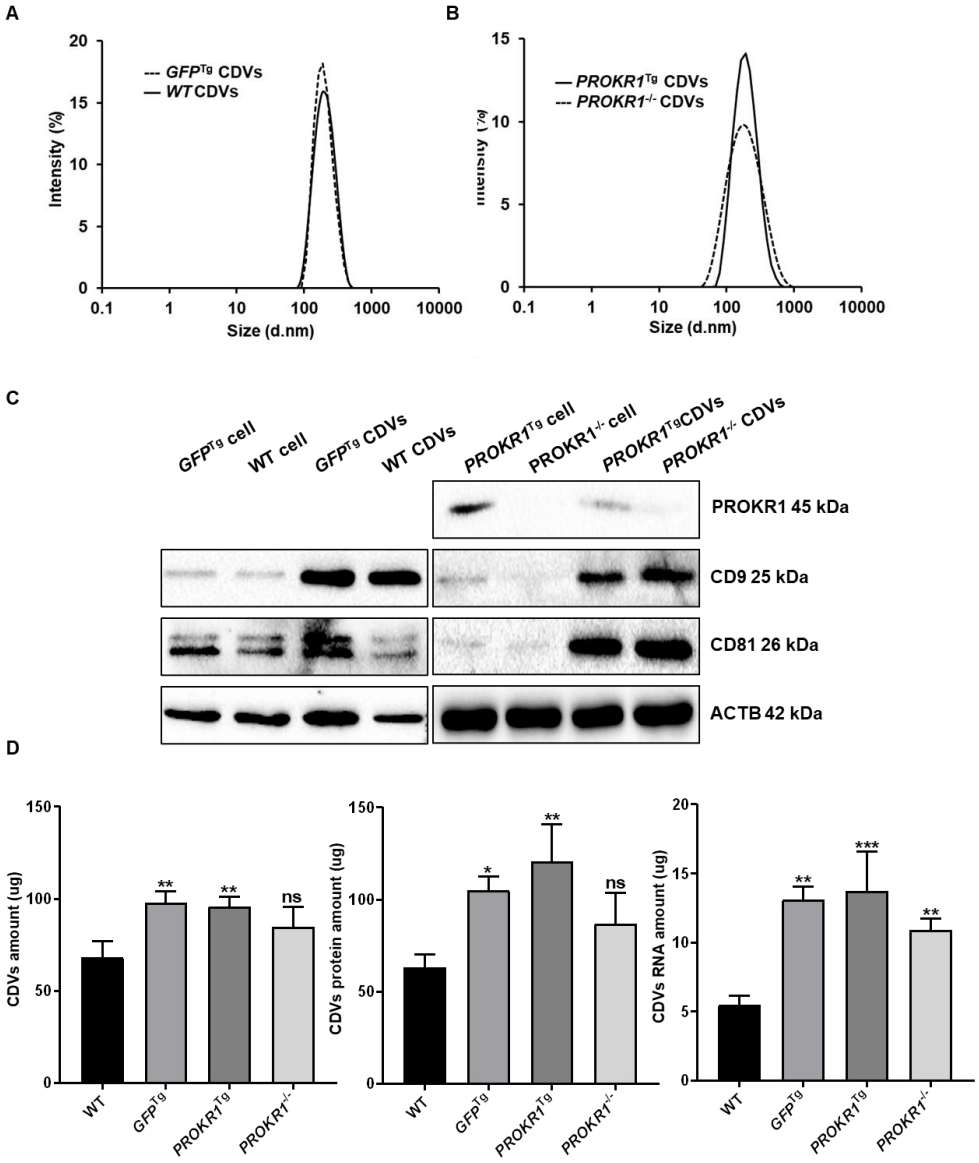
A
B
--- GFPTg CDVs
— WT CDVs
Intensity (%)
Size (d.nm)
— PROKR1Tg CDVs
--- PROKR1-/- CDVs
C
GFPTg cell
WT cell
GFPTg CDVs
WT CDVs
PROKR1Tg cell
PROKR1-/- cell
PROKR1TgCDVs
PROKR1-/- CDVs
PROKR1 45 kDa
CD9 25 kDa
CD81 26 kDa
ACTB 42 kDa
D
CDVs amount (ug)
CDVs protein amount (ug)
CDVs RNA amount (ug)
WT
GFPTg
PROKR1Tg
PROKR1-/-

Figure 9. Characterization of CDVs generated from genetically engineered HEK293T cells

A. Size measurement of *GFP*^{Tg} CDVs by dynamic light scattering analysis. The line represents the average of the triplicate measurements. Horizontal axis indicates the diameter of CDV (nm), vertical axis indicates the intensity of CDVs (%).

B. Size measurement of *PROKR1*^{Tg} CDVs by dynamic light scattering analysis. The line represents the average of the triplicate measurements. Horizontal axis indicates the diameter of CDVs (nm), vertical axis indicates the intensity of CDVs (%).

C. Western blot analyses of exosomal proteins. Left panel: exosomal protein expression in *GFP*^{Tg} cells and CDVs, and their wild type counterparts. Right panel: exosomal protein expression in *PROKR1*^{Tg} and *PROKR1*$^{-/-}$ cells and CDVs. Beta actin (ACTB) is used as a normalizer.

D. Quantification of amount, protein, and total RNA in CDVs generate from 10^7 cells. Bars indicate mean ± SD, N=3. *$p < 0.05$, **$p < 0.01$, and ***$p < 0.001$ vs. CDVs from wildtype HEK293T cells. One-sided Student's t-test.

3. Delivery of GFP protein and mRNA through CDVs

For production of HEK293T cells overexpressing PROKR1, a piggyBac vector expressing GFP simultaneously with PROKR1 was used. Therefore, tracking of GFP signal was used as a useful method to observe the target protein inside the CDVs and their migration to target cells. To this end, we produced mock control HEK293T cells only expressing GFP, and observed GFP signal in CDVs. The over-crowded mock CDVs (*GFP*^{Tg} CDVs) expressed a strong GFP signal, they were generated from *GFP* HEK293T cells of which the cytosol was in charge with green fluorescent protein. *GFP*^{Tg} CDVs can be detected from condensed CDVs under Cytation Cell Imaging Reader (Figure 10A). To verify CDVs can be internalized into target cells, 100 μg/ml *GFP*^{Tg} CDVs were treated to wildtype HEK293T cells for 24 hrs, and observe real-time uptake process. As the white arrowhead in the pictures shows that *GFP*^{Tg} CDVs penetrate the plasma membrane of target wildtype HEK293T cells at 18th hr after treatment. (Figure 10B). Other condensed *GFP*^{Tg} CDVs where close to cells uptake happen within 1 hr after treatment, and the fluorescence intensity of *GFP*^{Tg} CDVs in the wildtype HEK293T cells increase within early treatment duration. These observations demonstrate that *GFP*^{Tg} CDVs contain GFP proteins, and these proteins can enter into wildtype HEK293T cells through plasma membranes.

According to the PCR result, *GFP* mRNA exist in *GFP* HEK293T cells and *GFP*^{Tg} CDVs (Figure 10C). Additionally, the uptake of CDVs was

confirmed by the existence of mRNA from inside of CDVs. For this purpose, RNAs in *GFP*^{Tg} CDVs-treated wildtype HEK293T cells and non-treated wildtype HEK293T cells were isolated at different time points using trypsin-EDTA. Trypsin-EDTA ruled out the possibility of *GFP*^{Tg} CDVs adsorbing on the wildtype HEK293T cell surface. According to a result, *GFP* mRNA in *GFP*^{Tg} CDVs-treated wildtype HEK293T cells was found, while the non-treated wildtype HEK293T cells have no *GFP* band (Figure 10D). These results imply that *GFP* mRNA in CDVs can be delivered to wildtype 293T cells, and it can be maintained up to 48 hrs in wildtype 293T cells. These results confirmed that CDVs derived from genetically engineered cells successfully delivered proteins and mRNAs to target cells, and that they were maintained for a certain period of time in the cells.

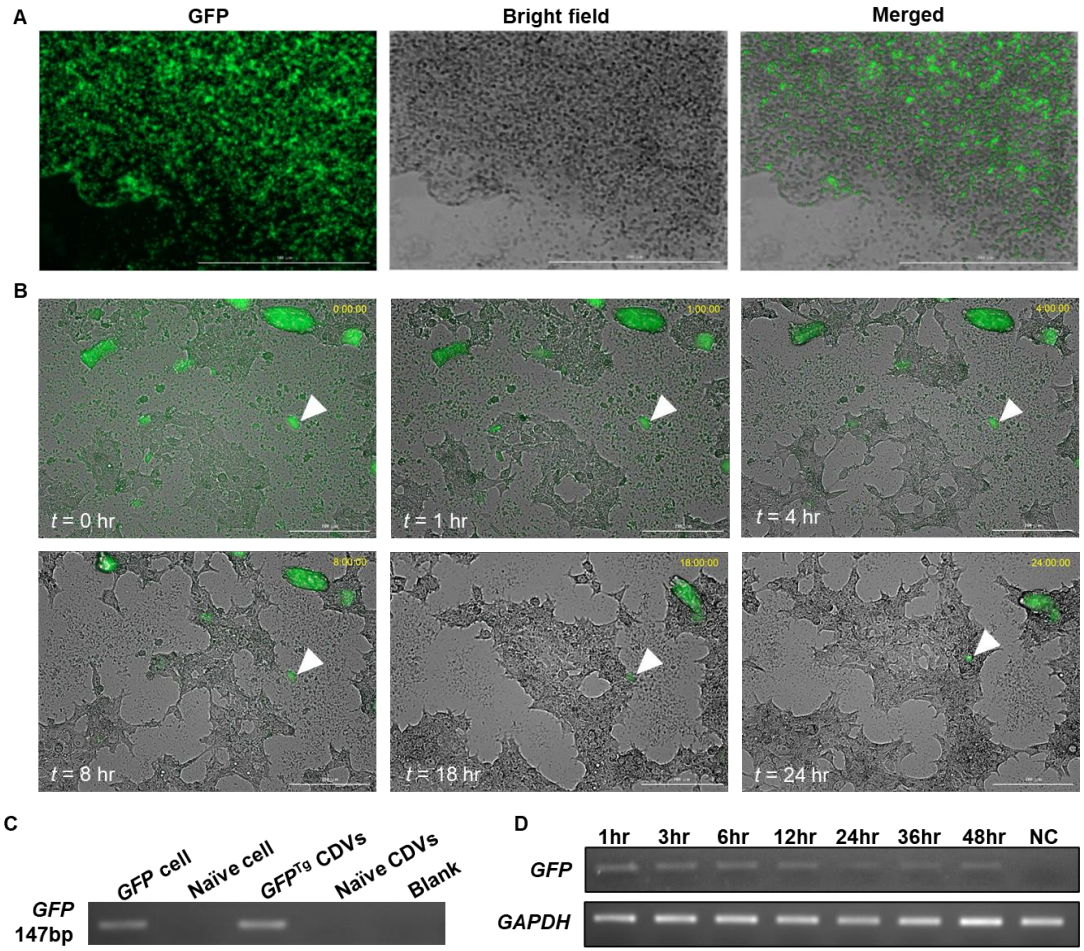
A
GFP
Bright field
Merged
B
t = 0 hr
t = 1 hr
t = 4 hr
t = 8 hr
t = 18 hr
t = 24 hr
C
GFP cell
Naïve cell
GFPrg CDVs
Naïve CDVs
Blank
GFP
147bp
D
1hr
3hr
6hr
12hr
24hr
36hr
48hr
NC
GFP
GAPDH

Figure 10. Delivery of GFP protein and mRNA through CDVs

A. Fluorescence image analysis of GFP protein inside the *GFP*^{Tg} CDVs. Left panel: CDVs under green fluorescence field. Middle panel: bright field. Right panel: merged image. Scale bar = 100 μm.

B. Real-time analysis of GFP protein delivery through *GFP*^{Tg} CDVs to wildtype HEK293T cells. Green fluorescence: *GFP*^{Tg} CDVs, t: time after CDVs treatment (hr), white arrowhead: representative *GFP*^{Tg} CDVs delivered to wildtype cell. Scale bar = 200 μm.

C. RT-PCR analysis of *GFP* mRNA in cells and CDVs. Gel image depicts the *GFP* mRNA expression in *GFP*^{Tg} and wildtype cells, CDVs from *GFP*^{Tg} and wildtype cells.

D. RT-PCR analysis of *GFP* mRNA in cells after *GFP*^{Tg} CDVs treatment. NC: wildtype HEK293T cells without *GFP* transgene. *GAPDH* is used as an internal control.

4. PROKR1 delivery to C2C12$^{Prokr1-/-}$ myoblasts

To investigate if the human PROKR1 protein can be delivered to mouse cells, western blotting was used. Wildtype C2C12 cells have PROKR1 protein expression. *Prokr1* successfully knockout in C2C12 myoblast cells were confirmed again. And only *PROKR1*^{Tg} CDVs-treated Prokr1 knock-out C2C12 myoblasts (C2C12$^{Prokr1-/-}$) myoblast cells have PROKR1 protein expression (Figure 11A). Which reveals that human gene *PROKR1* in *PROKR1*^{Tg} CDVs can be delivered to mouse C2C12$^{Prokr1-/-}$ myoblast cells successfully.

To find optimal *PROKR1*^{Tg} CDVs dose for treatment, different doses of *PROKR1*^{Tg} CDVs were tried, ranging from 10 to 200 μg/ml (Figure 11B). Cell proliferation reveals *PROKR1*^{Tg} CDVs toxicity to C2C12$^{Prokr1-/-}$ myoblast cells. *PROKR1*^{Tg} CDVs concentration at 100 μg/ml and 200 μg/ml treatment group decrease cell number by 69.29 % and 77.64 % respectively ($p < 0.001$) than non-treated of C2C12$^{Prokr1-/-}$ myoblast cells, and 200 μg/ml *PROKR1*^{Tg} CDVs had even severe toxicity to C2C12$^{Prokr1-/-}$ myoblast cells. Several smaller than 50 μg/ml *PROKR1*^{Tg} CDVs treatment groups showed increase C2C12$^{Prokr1-/-}$ myoblast cells proliferation capacity significantly, especially 25 μg/ml treatment group increase cell number by 25.2 % ($p < 0.001$) than the non-treated group of C2C12$^{Prokr1-/-}$ myoblast cells. Based on these results, the higher dose of *PROKR1*^{Tg} CDVs hinder cell proliferation, and the optimal concentration of *PROKR1*^{Tg} CDVs for treatment is 25 μg/ml.

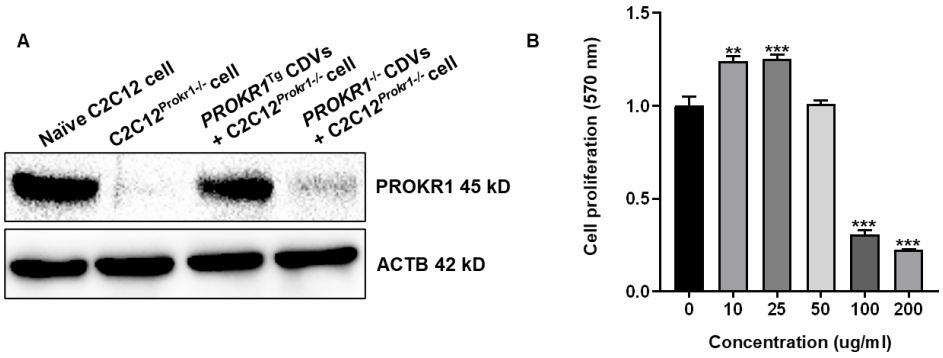

Figure 11. *PROKR1* delivery by *PROKR1*^{Tg} CDVs and dose range finding in C2C12$^{Prokr1-/-}$ myoblasts

A. Western blot analysis of PROKR1 in C2C12 myoblasts with or without CDVs treatment. Beta actin (ACTB) is used as an internal control.

B. Dose range finding of *PROKR1*^{Tg} CDVs MTT assay. Bars indicate mean ± SD, N=3. *p < 0.05; **p < 0.01; ***p < 0.001 vs. 0 μg/mL (vehicle control). One-sided Student's t-test.

5. Anti-apoptotic effect of *PROKR1*^{Tg} CDVs on C2C12$^{Prokr1-/-}$ myocytes

Wildtype C2C12 myoblast cells can differentiate into myocyte cells, but C2C12$^{Prokr1-/-}$ myoblast have severe apoptosis phenomenon at day 3. (Figure 12A). Compare non-treated C2C12$^{Prokr1-/-}$ myoblast cells, *PROKR1*^{Tg} CDVs treated C2C12$^{Prokr1-/-}$ myoblast cells show similar cell morphology with wildtype C2C12 myoblast cells, while *PROKR1*$^{-/-}$ CDVs treated C2C12$^{Prokr1-/-}$ myoblast cells still show severe apoptosis cell condition. Which reveals that can *PROKR1*^{Tg} CDVs alleviate C2C12$^{Prokr1-/-}$ apoptosis condition, but *PROKR1*$^{-/-}$ CDVs cannot achieve it.

To quantify C2C12$^{Prokr1-/-}$ apoptotic cells number, Flow cytometry analysis is used. *PROKR1*^{Tg} CDVs treated C2C12$^{Prokr1-/-}$ myocyte cells include 47.4±4.3% early apoptotic cells and 4.1±0.9% late apoptotic cells. *PROKR1*$^{-/-}$ CDVs treated C2C12$^{Prokr1-/-}$ myocyte cells have 36.8±1.9% early apoptotic cells and 6.3±0.2% late apoptotic cells (Figure 12B). Apoptotic cells were calculated by early and late apoptotic cells. Consistent early with the upper result (Figure 12A), after *PROKR1*^{Tg} CDVs treatment, C2C12$^{Prokr1-/-}$ myocyte apoptotic cells number decrease by 8.4% ($p < 0.05$) compare to the non-treated group.

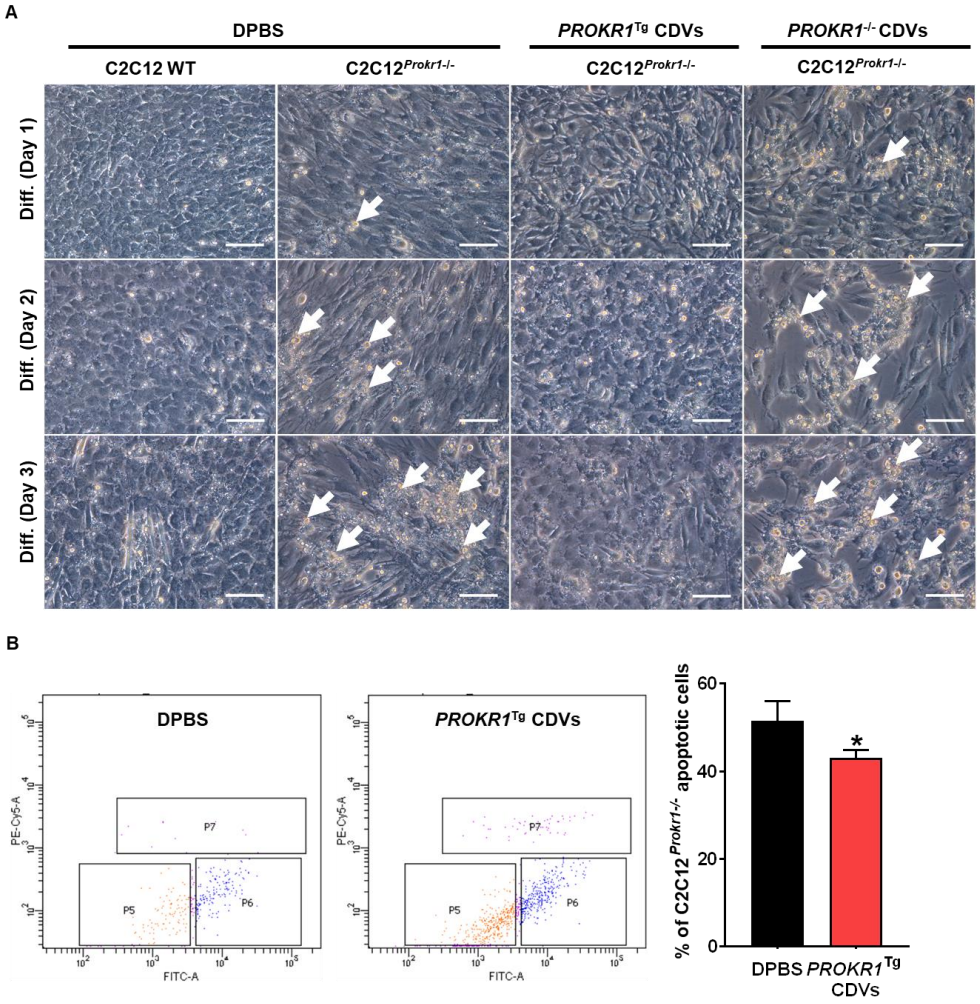
A
DPBS
PROKR1Tg CDVs
PROKR1-/- CDVs
C2C12 WT
C2C12Prokr1-/-
C2C12Prokr1-/-
C2C12Prokr1-/-
Diff. (Day 1)
Diff. (Day 2)
Diff. (Day 3)
B
DPBS
PROKR1Tg CDVs
PE-Cy5-A
FITC-A
P5
P6
P7
% of C2C12Prokr1-/- apoptotic cells
60
40
20
0
*
DPBS
PROKR1Tg CDVs

Figure 12. Anti-apoptotic effect of *PROKR1*^{Tg} CDVs on C2C12$^{Prokr1-/-}$ myocytes

A. Microscopic examination of C2C12$^{Prokr1-/-}$ myocytes after *PROKR1*^{Tg} CDVs treatment during differentiation. Diff: myogenic differentiation. White Arrows indicate floating cells. Scale bar = 100 μm.

B. Flow cytometry analysis of apoptotic C2C12$^{Prokr1-/-}$ myoblasts. Left panel: P5 fraction (orange) represents live cells, P6 (blue) represents annexin V-FITC (+)/PI (-) early apoptotic cells, P7 (purple) represents annexin V-FITC (+)/PI (-) late apoptotic cells. Right panel: gray bar indicates DPBS-treated C2C12$^{Prokr1-/-}$ myoblasts, red bars indicate *PROKR1*^{Tg} CDVs-treated C2C12$^{Prokr1-/-}$ myoblasts. Bars indicate mean ± SD, N = 3. *$p < 0.05$ vs. DPBS. One-sided Student's t-test.

6. Myogenic effect of *PROKR1*^{Tg} CDVs on C2C12$^{Prokr1-/-}$ myotubes

To investigate the differentiation effect of *PROKR1*^{Tg} CDVs on C2C12$^{Prokr1-/-}$, C2C12$^{Prokr1-/-}$ cells were incubated in the differentiation medium and CDVs medium for 6 days and then stained for Phalloidin and DAPI. Wildtype C2C12 myoblast cells can differentiate into myotube cells after differentiation 6 days. For C2C12$^{Prokr1-/-}$ cells, it has severe apoptotic condition and it cannot form myotube. But C2C12$^{Prokr1-/-}$ cells can form myotube in *PROKR1*^{Tg} CDVs treated medium after differentiation 6 days, while *PROKR1*$^{-/-}$ CDVs treatment group cannot recover the differentiation function of C2C12$^{Prokr1-/-}$ cells (Figure 13A). Which reveals that the *PROKR1* gene plays an important part role in C2C12 myoblast myogenesis process and *PROKR1*^{Tg} CDVs can recover C2C12$^{Prokr1-/-}$ cells differentiation function.

The expression of 6 genes associated with skeletal myogenesis of C2C12 cells treated *PROKR1*^{Tg} CDVs were analyzed using RT-PCR arrays. The fold change of up- and down-regulated genes in C2C12 cells and C2C12$^{Prokr1-/-}$ cells differentiated for 6 days was shown (Figure 13B), compared to undifferentiated group (p-value < 0.05). Wildtype C2C12 cells myotube marker (*Myh7, Myoglobin, Myog*) genes expression up-regulate at differentiation day 6. After *PROKR1*^{Tg} CDVs treatment, C2C12$^{Prokr1-/-}$ cells myotube marker genes up-regulate significantly. Especially *Myog* genes expression level in C2C12$^{Prokr1-/-}$ cells exceed over wildtype C2C12 cells.

Although *Myh7, Myoglobin* genes expression level in C2C12$^{Prokr1-/-}$ cells were lower than wildtype C2C12 cells. Wildtype C2C12 cells myoblast markers (*Pax3, Pax7, MyoD*) gene expression were down-regulated at differentiation day 6. After *PROKR1*^{Tg} CDVs treatment, C2C12$^{Prokr1-/-}$ cells *Pax3, Pax7, MyoD* gene expression up-regulate, which means C2C12$^{Prokr1-/-}$ cells can go to the reverse direction to reach the level of wildtype C2C12 cells gene expression. Based on these results it appears that the *PROKR1*^{Tg} CDVs can deliver *Prokr1* that regulates the skeletal myogenic fate of C2C12$^{Prokr1-/-}$ cells, resulting in the recovery of myogenic differentiation of C2C12$^{Prokr1-/-}$ cells.

To identify if C2C12$^{Prokr1-/-}$ cells-recovered myotubes have effect on insulin-stimulated glucose uptake, 2-NBDG as a substitute to measure glucose uptake level. Insulin activates 1.5 folds of glucose uptake compare to no insulin-treated wildtype C2C12 cells, and *PROKR1*^{Tg} CDVs and *PROKR1*$^{-/-}$ CDVs have no significant effect of glucose uptake in wildtype C2C12 cells (Figure 13C). C2C12$^{Prokr1-/-}$ cells have no insulin-accumulated glucose uptake effect. After *PROKR1*^{Tg} CDVs treatment, C2C12$^{Prokr1-/-}$ cells increase glucose uptake to 1.6 folds compare non-CDVs treated C2C12$^{Prokr1-/-}$ cells, and the glucose uptake level comparable with wildtype C2C12 cells. While *PROKR1*$^{-/-}$ CDVs treatment has no effect on C2C12$^{Prokr1-/-}$ cells glucose uptake level. These results indicate that *PROKR1*^{Tg} CDVs can recover myogenesis of C2C12$^{Prokr1-/-}$ cells and myotubes have glucose uptake function.

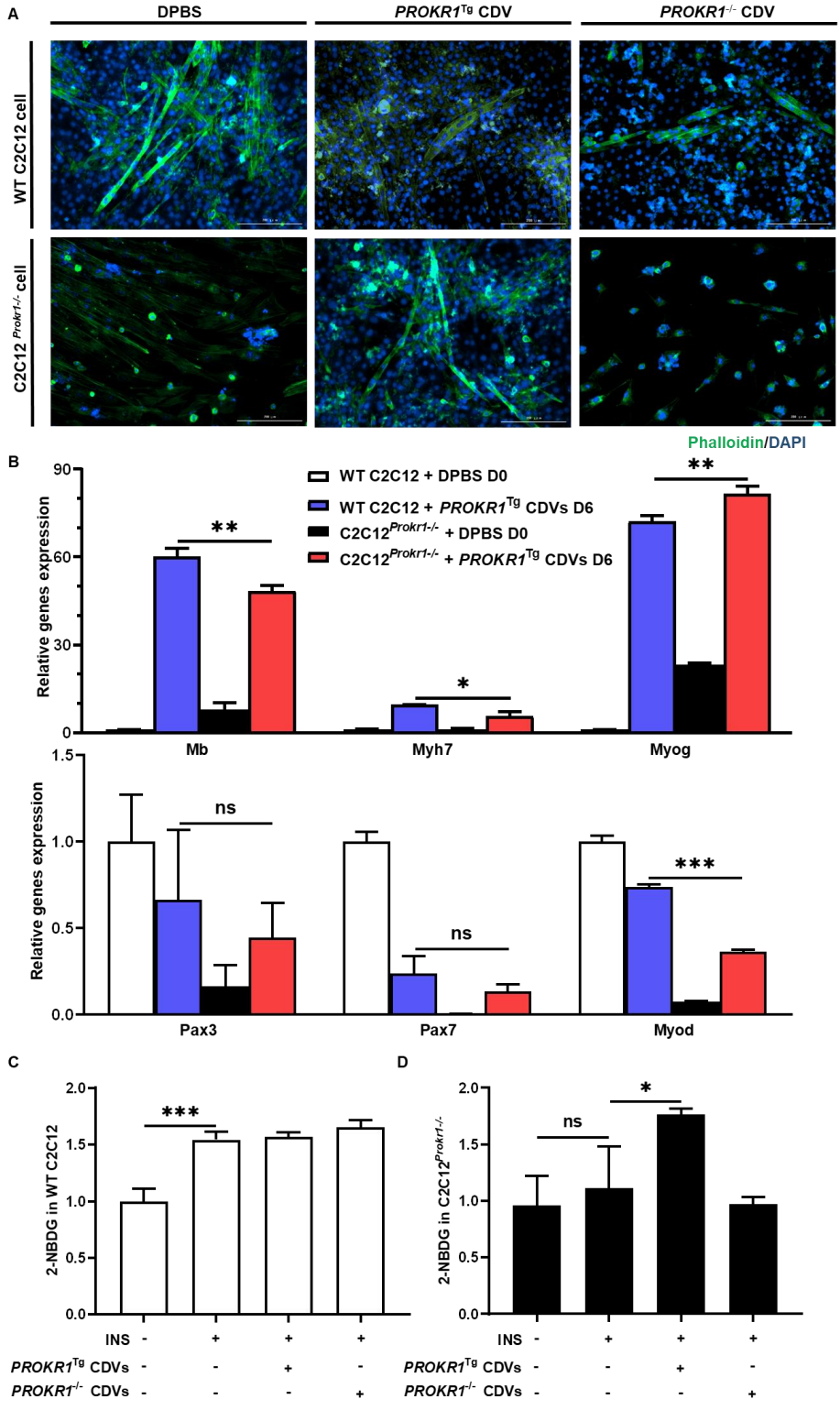
A
DPBS
PROKR1Tg CDV
PROKR1-/- CDV
WT C2C12 cell
C2C12 Prokr1-/- cell
Phalloidin/DAPI
B
WT C2C12 + DPBS D0
WT C2C12 + PROKR1Tg CDVs D6
C2C12Prokr1-/- + DPBS D0
C2C12Prokr1-/- + PROKR1Tg CDVs D6
Relative genes expression
Mb
Myh7
Myog
Pax3
Pax7
Myod
ns
C
2-NBDG in WT C2C12
D
2-NBDG in C2C12Prokr1-/-
INS
PROKR1Tg CDVs
PROKR1-/- CDVs

Figure 13. Myogenic effect of *PROKR1*^{Tg} CDVs on C2C12$^{Prokr1-/-}$ myotubes

A. Microscopic examination of C2C12$^{Prokr1-/-}$ myotubes at differentiation day 6. Green: Phalloidin staining on actin filaments, blue: DAPI staining on nuclei. Scale bar = 200 μm.

B. RT-PCR analysis of early and late myogenic markers. Black bars indicate DPBS-treated wildtype C2C12 myoblasts before differentiation. Bars indicate mean ± SD, N = 3. *p < 0.05, **p < 0.01, ***p < 0.001, ns: not significant. One-sided Student's t-test.

C. Insulin-stimulated glucose uptake in wildtype C2C12 myotubes. Black bars indicate non-treated wildtype C2C12 myotubes. Bars indicate mean ± SD. N = 3. *p < 0.05, ns: not significant. One-sided Student's t-test. INS: insulin.

D. Insulin-stimulated glucose uptake in C2C12$^{Prokr1-/-}$-derived myotubes. Gray bars indicate C2C12$^{Prokr1-/-}$ cells. Bars indicate mean ± SD. N = 3. *p < 0.05, ns: not significant. One-sided Student's t-test. INS: insulin.

Discussion

CDVs, an artificial type of exosomes strategies which are generated by passing cells through micro-sized pores have been established in recent years, could efficiently deliver siRNA and mRNA to recipient cells and have some characteristics similar to exosomes [64, 99]. In this study, CDVs showed to have similar size distribution and marker expression as exosomes such as CD9 and CD81, and a higher yield of preparation than exosomes (Figure 9). In addition, RNA profile of CDVs were similar to typical RNA profiles of cells and tissues having 2:1 ratio of 18S rRNA:28S rRNA (Figure 8C). Since the loading process of the proteins and RNAs into CDVs was a mechanical burst and enclosure of cells without any chemical or enzymatic treatment, the overall quality of the proteins and RNAs in the CDVs was well preserved [72]. The unique protein on the exosome surface is regarded responsible to tumor-specific binding. Recently, doxorubicin-loaded CDVs also have been proved to bind tumor cells specifically in animals [65].

Prokr1 has been known to play a vital part in various tissues by suppressing of preadipocyte differentiation and proliferation [79], improving insulin sensitivity and cardiac protection [93], and kidney development and function [92]. Although many studies reveal the metabolic functions of *Prokr1*, the function of *Prokr1* in skeletal muscle is still unknown. Here, the therapeutic effect of Prokr1 was evaluated by delivery of PROKR1 protein through CDVs to rescue the myogenic potential of Prokr1 deleted C2C12 cells. To be sure of

successful delivery of Prokr1, GFP delivery as an alternative method was visually confirmed (Figure 10B). Many groups use fluorescence dye to confirm CDV uptake. For example, CDVs labeled with PKH67 [100], and exosome labeled with DIC [101] have been observed taken up into recipient cells. But this conclusion does not hold if fluorescence is not tightly coupled with CDVs, then only fluorescence without CDVs could be observed. Green fluorescence from GFP inside the *GFP*^{Tg} CDVs ruled out this possibility, and verified that the fluorescence came out from CDVs, and they were successfully internalized in the recipient cells.

PROKR1^{Tg} CDVs dose for C2C12$^{Prokr1-/-}$ myoblast cells were confirmed (Figure 11B). As the nanovesicles are enclosed by a lipid layer, the generated CDVs would have lipid-induced toxicity [72, 102]. The cell viability of CDVs treated samples was high when the CDVs concentration were 10-25 μg/ml, but low when it is 100-200 μg/ml. We hypothesize that a certain amount of CDVs could precede cell proliferation [72] and migration [103, 104], while the excessive amount of CDVs might impede cell proliferation. The reduced cell proliferation may be related to lipid-induced toxicity, which hindered material transportation in the recipient cell membranes [105]. Moreover, excessive CDVs limits uptake by recipient cells because the uptake needs ATP [106].

Apply *PROKR1*^{Tg} and *PROKR1*$^{-/-}$ CDVs to C2C12$^{Prokr1-/-}$ myocyte cells, only *PROKR1*^{Tg} CDVs anti-apoptosis effect has appeared (Figure 12A, B). We hypothesize that *PROKR1* is an indispensable part in the process of wildtype C2C12 cell differentiation, and *PROKR1*^{Tg} CDVs can make up for the

molecular mechanism of the C2C12$^{Prokr1-/-}$ cell, thereby improving the apoptosis state of the cell. CDVs were found to contain abundant amount of Bcl-2 [107], and C2C12 differentiating cells have Bcl-2-dependent mechanism, accompanied by enhanced apoptosis in Bcl-2 deficient myotubes [108]. In addition, it has been shown that the overexpression of Bcl2 protects immortalized cells against chemical-induced cell death [109]. Overall, CDVs could be helpful as a potential anti-apoptosis agent.

We hypothesized that *PROKR1*^{Tg} CDVs loaded with overexpressed *PROKR1* and it can regulate myogenesis of C2C12$^{Prokr1-/-}$ cell. Several groups have addressed that exosomal factors derived from various cell contribute differentiation of cells. For example, exosomes of cancer cells contain TGF-β1 induce the differentiation of Adipose-Derived Stem Cells (ASCs) and Mesenchymal Stem Cells (MSCs) into fibroblast cells [110, 111]. And exosomes from differentiating human skeletal muscle cells trigger myogenesis of stem cells and provide myogenic growth factors related to muscle regeneration [101]. We found that *PROKR1*^{Tg} CDVs contribute to myogenic differentiation of C2C12$^{Prokr1-/-}$ cells (Figure 13A, B). Stimulation by *PROKR1*^{Tg} CDVs significantly altered the morphological phenotype of C2C12$^{Prokr1-/-}$ cells, while *PROKR1*$^{-/-}$ CDVs cannot achieve it (Figure 13A). Moreover, mRNA expression of myogenic gene such as *Myh7, Myoglobin, Myogenin, Pax3, Pax7* and *MyoD* are related to myogenic differentiation, was increased in C2C12$^{Prokr1-/-}$ cells by CDVs over 6 days, which regulate myogenic marker level of C2C12$^{Prokr1-/-}$ cells similar with wildtype C2C12

cells (Figure 13B). Imperfectly, most of C2C12$^{Prokr1-/-}$ cells were in apoptotic and dead state at differentiation day 6, so it is hard to harvest C2C12$^{Prokr1-/-}$ cells and get the high amount and quality RNA of non-treated C2C12$^{Prokr1-/-}$ cells (Figure 13B). Other groups demonstrate that *PROKR1* act as paracrine factor to trigger the differentiation of epicardial-derived progenitor cells (EPDC) [91]. *PROKR1* has been shown to induce the differentiation of monocytes into macrophage-like cells with morphological changes [112]. It is revealed that *PROKR1* plays an important part role in various cell types. Therefore, these results support our hypothesis that *PROKR1* can be efficiently delivered into C2C12$^{Prokr1-/-}$ cells and may trigger myogenic signaling pathways, resulting in skeletal myogenic differentiation.

We also investigate the insulin-stimulated glucose uptake effect of differentiating myotube of wildtype C2C12 and C2C12$^{Prokr1-/-}$ cells. Skeletal muscle is a major organ responsible for maintaining whole body glucose homeostasis and insulin-stimulated glucose uptake [113]. Glucose uptake in skeletal muscle is mediated by insulin. The insulin can activate phosphoinositide 3-kinase (PI3K)/protein kinase B (AKT) signaling pathway through phosphorylates Insulin-Receptor Substrate (IRS) [95]. AKT is responsible for activating translocate Glucose transporter type 4 (Glut4) to induce the traffic of Glut4-containing vesicles to the plasma membrane [114, 115]. As result shows that insulin promotes glucose uptake in wildtype C2C12 cells, but in C2C12$^{Prokr1-/-}$ cells, insulin signaling were impaired (Figure 13C). Insulin impairment of C2C12$^{Prokr1-/-}$ cells seems to be caused by defects in the

PI3K/Akt signaling pathway, resulting in reduction of Glut4 translocation. After *PROKR1*^{Tg} CDVs treatment, the glucose uptake level of C2C12$^{Prokr1-/-}$ cells is recovered, comparable with wildtype C2C12 cells (Figure 13C). *Prokr1* activation increase Glut4 translocation, glucose uptake and insulin sensitivity through activation of the PI3K/Akt pathway in skeletal muscle [98]. Thus, we can consider that due to the *PROKR1*^{Tg} CDVs, C2C12$^{Prokr1-/-}$ myoblast cells can differentiate to myotubes, and these myotubes have insulin-stimulated glucose uptake effect by activation of the PI3K/Akt pathway.

However, more studies should be performed in vivo to further investigate the potential of *Prokr1* to be used to regulate insulin resistance and myogenesis. In the next step, the effect of *PROKR1*^{Tg} CDVs on fast twitch muscle fiber is remained to be clarified. The therapeutic potential of *PROKR1*^{Tg} CDVs on age-related sarcopenia and/or muscle-related metabolic disorders is worthy to be addressed. It reveals that myotube of *PROKR1*^{Tg} CDVs-treated C2C12$^{Prokr1-/-}$ cells have a normal physiological function.

Conclusion

These results demonstrated that *PROKR1*^{Tg} CDVs would deliver PROKR1 protein to C2C12$^{Prokr1-/-}$ myoblasts, reduce apoptosis of C2C12$^{Prokr1-/-}$-derived myocytes, and eventually rescue the morphological and functional development of C2C12$^{Prokr1-/-}$-derived myotubes. Although the exact mechanism for the myogenic effect of PROKR1 remain unknown, *PROKR1*^{Tg} CDVs appear to recover C2C12$^{Prokr1-/-}$ cells for differentiation by transfer PROKR1 membrane protein, thereby regulate C2C12$^{Prokr1-/-}$ cells fate towards myotubes accompanied with the capacity of insulin-stimulated glucose uptake. Therefore, *PROKR1*^{Tg} CDVs would provide a new approach for skeletal muscle differentiation.

Reference

1. Kalra, H., G.P. Drummen, and S. Mathivanan, *Focus on Extracellular Vesicles: Introducing the Next Small Big Thing.* Int J Mol Sci, 2016. **17**(2): p. 170.
2. Bunggulawa, E.J., et al., *Recent advancements in the use of exosomes as drug delivery systems.* J Nanobiotechnology, 2018. **16**(1): p. 81.
3. Marote, A., et al., *MSCs-Derived Exosomes: Cell-Secreted Nanovesicles with Regenerative Potential.* Front Pharmacol, 2016. **7**: p. 231.
4. Armstrong, D. and D.E. Wildman, *Extracellular Vesicles and the Promise of Continuous Liquid Biopsies.* J Pathol Transl Med, 2018. **52**(1): p. 1-8.
5. Han, Y., et al., *Salivary Exosomes: Emerging Roles in Systemic Disease.* Int J Biol Sci, 2018. **14**(6): p. 633-643.
6. Thery, C., et al., *Isolation and characterization of exosomes from cell culture supernatants and biological fluids.* Curr Protoc Cell Biol, 2006. **Chapter 3**: p. Unit 3.22.
7. Kowal, J., et al., *Proteomic comparison defines novel markers to characterize heterogeneous populations of extracellular vesicle subtypes.* Proc Natl Acad Sci U S A, 2016. **113**(8): p. E968-77.
8. Edgar, J.R., *Q&A: What are exosomes, exactly?* BMC Biol, 2016. **14**: p. 46.
9. Whitehead, C.A., et al., *Cancer exosomes in cerebrospinal fluid.* 2017. **6**(8): p. s1352-s1370.
10. Klumperman, J. and G. Raposo, *The complex ultrastructure of the endolysosomal system.* Cold Spring Harb Perspect Biol, 2014. **6**(10): p. a016857.
11. Stoorvogel, W., et al., *Late endosomes derive from early endosomes by maturation.* 1991. **65**(3): p. 417-427.
12. Gruenberg, J. and F.G. van der Goot, *Mechanisms of pathogen entry through the endosomal compartments.* Nat Rev Mol Cell Biol, 2006. **7**(7): p. 495-504.
13. van Niel, G., et al., *Exosomes: a common pathway for a specialized function.* J Biochem, 2006. **140**(1): p. 13-21.
14. Record, M., et al., *Exosomes as intercellular signalosomes and pharmacological effectors.* Biochem Pharmacol, 2011. **81**(10): p. 1171-82.

15. Bilodeau, P.S., et al., *The Vps27p–Hse1p complex binds ubiquitin and mediates endosomal protein sorting.* 2002. **4**(7): p. 534-539.
16. Shields, S.B., et al., *ESCRT ubiquitin-binding domains function cooperatively during MVB cargo sorting.* 2009. **185**(2): p. 213-224.
17. Henne, W.M., N.J. Buchkovich, and S.D. Emr, *The ESCRT pathway.* Dev Cell, 2011. **21**(1): p. 77-91.
18. Wollert, T. and J.H. Hurley, *Molecular mechanism of multivesicular body biogenesis by ESCRT complexes.* Nature, 2010. **464**(7290): p. 864-9.
19. Shields, S.B. and R.C. Piper, *How ubiquitin functions with ESCRTs.* Traffic, 2011. **12**(10): p. 1306-17.
20. Goni, F.M. and A. Alonso, *Biophysics of sphingolipids I. Membrane properties of sphingosine, ceramides and other simple sphingolipids.* Biochim Biophys Acta, 2006. **1758**(12): p. 1902-21.
21. Gurunathan, S., et al., *Review of the isolation, characterization, biological function, and multifarious therapeutic approaches of exosomes.* 2019. **8**(4): p. 307.
22. Hessvik, N.P. and A. Llorente, *Current knowledge on exosome biogenesis and release.* Cell Mol Life Sci, 2018. **75**(2): p. 193-208.
23. Hessvik, N.P. and A. Llorente, *Current knowledge on exosome biogenesis and release.* Cellular and molecular life sciences : CMLS, 2018. **75**(2): p. 193-208.
24. Savina, A., et al., *Rab11 promotes docking and fusion of multivesicular bodies in a calcium-dependent manner.* Traffic, 2005. **6**(2): p. 131-43.
25. Ostrowski, M., et al., *Rab27a and Rab27b control different steps of the exosome secretion pathway.* Nat Cell Biol, 2010. **12**(1): p. 19-30; sup pp 1-13.
26. Urbanelli, L., et al., *Signaling pathways in exosomes biogenesis, secretion and fate.* Genes, 2013. **4**(2): p. 152-170.
27. Fader, C.M., et al., *TI-VAMP/VAMP7 and VAMP3/cellubrevin: two v-SNARE proteins involved in specific steps of the autophagy/multivesicular body pathways.* Biochim Biophys Acta, 2009. **1793**(12): p. 1901-16.
28. Gonda, A., et al., *Cellular-Defined Microenvironmental Internalization of Exosomes*, in *Extracellular Vesicles*. 2019, IntechOpen.

29. Mulcahy, L.A., R.C. Pink, and D.R. Carter, *Routes and mechanisms of extracellular vesicle uptake.* J Extracell Vesicles, 2014. **3**.
30. Montecalvo, A., et al., *Mechanism of transfer of functional microRNAs between mouse dendritic cells via exosomes.* 2012. **119**(3): p. 756-766.
31. Platt, C.D., et al., *Mature dendritic cells use endocytic receptors to capture and present antigens.* Proc Natl Acad Sci U S A, 2010. **107**(9): p. 4287-92.
32. Takano, M., et al., *Receptor-mediated endocytosis of macromolecules and strategy to enhance their transport in alveolar epithelial cells.* Expert opinion on drug delivery, 2015. **12**(5): p. 813-825.
33. Asmat, T.M., et al., *Endocytosis of Streptococcus pneumoniae via the polymeric immunoglobulin receptor of epithelial cells relies on clathrin and caveolin dependent mechanisms.* 2014. **304**(8): p. 1233-1246.
34. Kalluri, R. and V.S.J.S. LeBleu, *The biology, function, and biomedical applications of exosomes.* 2020. **367**(6478).
35. Escrevente, C., et al., *Interaction and uptake of exosomes by ovarian cancer cells.* 2011. **11**(1): p. 108.
36. Yang, Z., et al., *Functional exosome-mimic for delivery of siRNA to cancer: in vitro and in vivo evaluation.* J Control Release, 2016. **243**: p. 160-171.
37. Chen, C.C., et al., *Elucidation of Exosome Migration across the Blood-Brain Barrier Model In Vitro.* Cellular and molecular bioengineering, 2016. **9**(4): p. 509-529.
38. Yuan, D., et al., *Macrophage exosomes as natural nanocarriers for protein delivery to inflamed brain.* 2017. **142**: p. 1-12.
39. Yang, Y.-G., et al., *Tetraspanins: Spanning from solid tumors to hematologic malignancies.* 2016. **44**(5): p. 322-328.
40. Pols, M.S. and J.J.E.c.r. Klumperman, *Trafficking and function of the tetraspanin CD63.* 2009. **315**(9): p. 1584-1592.
41. Luga, V., et al., *Exosomes mediate stromal mobilization of autocrine Wnt-PCP signaling in breast cancer cell migration.* 2012. **151**(7): p. 1542-1556.
42. Shao, Y., et al., *The functions and clinical applications of tumor-derived exosomes.* 2016. **7**(37): p. 60736.
43. Yang, S.-j., et al., *Predictive role of GSTP1-containing exosomes in chemotherapy-resistant breast cancer.* 2017. **623**: p. 5-14.

44. Koga, K., et al., *Purification, characterization and biological significance of tumor-derived exosomes.* 2005. **25**(6A): p. 3703-3707.
45. Chen, Y., et al., *Exosomal microRNA miR-92a concentration in serum reflects human brown fat activity.* Nature Communications, 2016. **7**(1): p. 11420.
46. Shi, J., *Considering Exosomal miR-21 as a Biomarker for Cancer.* J Clin Med, 2016. **5**(4).
47. Zhuang, X., et al., *Treatment of brain inflammatory diseases by delivering exosome encapsulated anti-inflammatory drugs from the nasal region to the brain.* Mol Ther, 2011. **19**(10): p. 1769-79.
48. Yang, T., et al., *Exosome delivered anticancer drugs across the blood-brain barrier for brain cancer therapy in Danio rerio.* 2015. **32**(6): p. 2003-2014.
49. Aminzadeh, M.A., et al., *Reversal of cardiac and skeletal manifestations of Duchenne muscular dystrophy by cardiosphere-derived cells and their exosomes in mdx dystrophic mice and in human Duchenne cardiomyocytes.* 2017: p. 128900.
50. Akers, J.C., et al., *Optimizing preservation of extracellular vesicular miRNAs derived from clinical cerebrospinal fluid.* 2016. **17**(2): p. 125-132.
51. Teixeira, J.H., et al., *Circulating extracellular vesicles: Their role in tissue repair and regeneration.* Transfus Apher Sci, 2016. **55**(1): p. 53-61.
52. Robbins, P.D. and A.E. Morelli, *Regulation of immune responses by extracellular vesicles.* Nat Rev Immunol, 2014. **14**(3): p. 195-208.
53. Wang, J., Y. Zheng, and M. Zhao, *Exosome-Based Cancer Therapy: Implication for Targeting Cancer Stem Cells.* Front Pharmacol, 2016. **7**: p. 533.
54. Luan, X., et al., *Engineering exosomes as refined biological nanoplatforms for drug delivery.* Acta Pharmacol Sin, 2017. **38**(6): p. 754-763.
55. Inamdar, S., R. Nitiyanandan, and K. Rege, *Emerging applications of exosomes in cancer therapeutics and diagnostics.* Bioengineering & translational medicine, 2017. **2**(1): p. 70-80.
56. Banizs, A.B., et al., *In vitro evaluation of endothelial exosomes as carriers for small interfering ribonucleic acid delivery.* Int J Nanomedicine, 2014. **9**: p. 4223-30.

57. Besse, B., et al., *Dendritic cell-derived exosomes as maintenance immunotherapy after first line chemotherapy in NSCLC.* 2016. **5**(4): p. e1071008.
58. Kordelas, L., et al., *MSC-derived exosomes: a novel tool to treat therapy-refractory graft-versus-host disease.* 2014. **28**(4): p. 970-973.
59. Marban, E., *The Secret Life of Exosomes: What Bees Can Teach Us About Next-Generation Therapeutics.* J Am Coll Cardiol, 2018. **71**(2): p. 193-200.
60. Zhu, Q., et al., *Microfluidic engineering of exosomes: editing cellular messages for precision therapeutics.* Lab Chip, 2018. **18**(12): p. 1690-1703.
61. Jo, W., et al., *Large-scale generation of cell-derived nanovesicles.* Nanoscale, 2014. **6**(20): p. 12056-64.
62. Goh, W.J., et al., *Bioinspired Cell-Derived Nanovesicles versus Exosomes as Drug Delivery Systems: a Cost-Effective Alternative.* Sci Rep, 2017. **7**(1): p. 14322.
63. Antimisiaris, S.G., S. Mourtas, and A. Marazioti, *Exosomes and Exosome-Inspired Vesicles for Targeted Drug Delivery.* Pharmaceutics, 2018. **10**(4).
64. Wu, J.-Y., et al., *Exosome-Mimetic Nanovesicles from Hepatocytes promote hepatocyte proliferation in vitro and liver regeneration in vivo.* 2018. **8**(1): p. 1-11.
65. Jang, S.C., et al., *Bioinspired exosome-mimetic nanovesicles for targeted delivery of chemotherapeutics to malignant tumors.* 2013. **7**(9): p. 7698-7710.
66. Yoon, J., et al., *Generation of nanovesicles with sliced cellular membrane fragments for exogenous material delivery.* Biomaterials, 2015. **59**: p. 12-20.
67. Goh, W.J., et al., *Doxorubicin-loaded cell-derived nanovesicles: an alternative targeted approach for anti-tumor therapy.* International journal of nanomedicine, 2017. **12**: p. 2759-2767.
68. Kalimuthu, S., et al., *A New Approach for Loading Anticancer Drugs Into Mesenchymal Stem Cell-Derived Exosome Mimetics for Cancer Therapy.* 2018. **9**(1116).

69. Lunavat, T.R., et al., *RNAi delivery by exosome-mimetic nanovesicles - Implications for targeting c-Myc in cancer.* Biomaterials, 2016. **102**: p. 231-8.
70. *<Bioinspired Exosome Mimetic Nanovesicles for Targeted Delivery of Chemotherapeutics toMalignant Tumors.pdf>.*
71. Hwang, D.W., et al., *Noninvasive imaging of radiolabeled exosome-mimetic nanovesicle using 99mTc-HMPAO.* Scientific Reports, 2015. **5**(1): p. 15636.
72. Jeong, D., et al., *Nanovesicles engineered from ES cells for enhanced cell proliferation.* Biomaterials, 2014. **35**(34): p. 9302-10.
73. Zhu, L., et al., *Novel alternatives to extracellular vesicle-based immunotherapy - exosome mimetics derived from natural killer cells.* Artif Cells Nanomed Biotechnol, 2018. **46**(sup3): p. S166-s179.
74. Kalimuthu, S., et al., *In Vivo therapeutic potential of mesenchymal stem cell-derived extracellular vesicles with optical imaging reporter in tumor mice model.* Scientific Reports, 2016. **6**(1): p. 30418.
75. Leney, S.E. and J.M. Tavaré, *The molecular basis of insulin-stimulated glucose uptake: signalling, trafficking and potential drug targets.* The Journal of endocrinology, 2009. **203**(1): p. 1-18.
76. Reaven, G.M., et al., *Measurement of plasma glucose, free fatty acid, lactate, and insulin for 24 h in patients with NIDDM.* Diabetes, 1988. **37**(8): p. 1020-4.
77. Ganz, M.L., et al., *The association of body mass index with the risk of type 2 diabetes: a case–control study nested in an electronic health records system in the United States.* Diabetology & Metabolic Syndrome, 2014. **6**(1): p. 50.
78. Balistreri, C.R., C. Caruso, and G.J.M.o.i. Candore, *The role of adipose tissue and adipokines in obesity-related inflammatory diseases.* 2010. **2010**.
79. Szatkowski, C., et al., *Prokineticin receptor 1 as a novel suppressor of preadipocyte proliferation and differentiation to control obesity.* PLoS One, 2013. **8**(12): p. e81175.
80. Beale, K., et al., *Peripheral administration of prokineticin 2 potently reduces food intake and body weight in mice via the brainstem.* Br J Pharmacol, 2013. **168**(2): p. 403-10.

81. Genders, A.J., et al., *Endothelial cells actively concentrate insulin during its transendothelial transport.* Microcirculation, 2013. **20**(5): p. 434-9.
82. Soga, T., et al., *Molecular cloning and characterization of prokineticin receptors.* 2002. **1579**(2-3): p. 173-179.
83. Cao, Y.J.C.m., *Angiogenesis and vascular functions in modulation of obesity, adipose metabolism, and insulin sensitivity.* 2013. **18**(4): p. 478-489.
84. Dormishian, M., et al., *Prokineticin receptor-1 is a new regulator of endothelial insulin uptake and capillary formation to control insulin sensitivity and cardiovascular and kidney functions.* J Am Heart Assoc, 2013. **2**(5): p. e000411.
85. Nebigil, C.G.J.F.i.c.m., *Prokineticin is a new linker between obesity and cardiovascular diseases.* 2017. **4**: p. 20.
86. Podlovni, H., et al., *Differential expression of prokineticin receptors by endothelial cells derived from different vascular beds: a physiological basis for distinct endothelial function.* Cell Physiol Biochem, 2006. **18**(6): p. 315-26.
87. Guilini, C., et al., *Divergent roles of prokineticin receptors in the endothelial cells: angiogenesis and fenestration.* Am J Physiol Heart Circ Physiol, 2010. **298**(3): p. H844-52.
88. Urayama, K., et al., *Prokineticin receptor-1 induces neovascularization and epicardial-derived progenitor cell differentiation.* 2008. **28**(5): p. 841-849.
89. Kubota, T., et al., *Impaired insulin signaling in endothelial cells reduces insulin-induced glucose uptake by skeletal muscle.* 2011. **13**(3): p. 294-307.
90. Nebigil, C.G.J.H., *Updates on Endothelial Functions of Proangiogenic Prokineticin.* 2016. **68**(5): p. 1091-1097.
91. Urayama, K., et al., *Prokineticin receptor-1 induces neovascularization and epicardial-derived progenitor cell differentiation.* Arterioscler Thromb Vasc Biol, 2008. **28**(5): p. 841-9.
92. Boulberdaa, M., et al., *Genetic inactivation of prokineticin receptor-1 leads to heart and kidney disorders.* 2011. **31**(4): p. 842-850.
93. Urayama, K., et al., *The prokineticin receptor-1 (GPR73) promotes cardiomyocyte survival and angiogenesis.* Faseb j, 2007. **21**(11): p. 2980-93.

94. Krook, A., et al., *Insulin-stimulated Akt kinase activity is reduced in skeletal muscle from NIDDM subjects.* 1998. **47**(8): p. 1281-1286.
95. Niswender, K.D., et al., *Insulin activation of phosphatidylinositol 3-kinase in the hypothalamic arcuate nucleus: a key mediator of insulin-induced anorexia.* 2003. **52**(2): p. 227-231.
96. Parker, R., et al., *Y-receptor-like genes GPR72 and GPR73: molecular cloning, genomic organisation and assignment to human chromosome 11q21.1 and 2p14 and mouse chromosome 9 and 6.* Biochimica et biophysica acta, 2000. **1491**(1-3): p. 369-375.
97. Von Hunolstein, J.J. and C.G. Nebigil, *Can prokineticin prevent obesity and insulin resistance?* Curr Opin Endocrinol Diabetes Obes, 2015. **22**(5): p. 367-73.
98. Jongsoo, M. and J. Park, *Prokineticin Receptor 1 Activation Induces Myogenesis and Ameliorates Insulin Resistance in Mouse Skeletal Muscle Cells*. 2018, Am Diabetes Assoc.
99. Lunavat, T.R., et al., *RNAi delivery by exosome-mimetic nanovesicles–Implications for targeting c-Myc in cancer.* 2016. **102**: p. 231-238.
100. Wu, J.Y., et al., *Exosome-Mimetic Nanovesicles from Hepatocytes promote hepatocyte proliferation in vitro and liver regeneration in vivo.* Sci Rep, 2018. **8**(1): p. 2471.
101. Choi, J.S., et al., *Exosomes from differentiating human skeletal muscle cells trigger myogenesis of stem cells and provide biochemical cues for skeletal muscle regeneration.* J Control Release, 2016. **222**: p. 107-15.
102. Petersen, S., et al., *The physical state of lipid nanoparticles influences their effect on in vitro cell viability.* Eur J Pharm Biopharm, 2011. **79**(1): p. 150-61.
103. Brown, M., et al., *Lymphatic exosomes promote dendritic cell migration along guidance cues.* 2018. **217**(6): p. 2205-2221.
104. Midwood, K.S., et al., *Tissue repair and the dynamics of the extracellular matrix.* 2004. **36**(6): p. 1031-1037.
105. Zepik, H.H., et al., *Lipid vesicles as membrane models for toxicological assessment of xenobiotics.* 2008. **38**(1): p. 1-11.

106. Ronquist, K.G., et al., *Energy-requiring uptake of prostasomes and PC3 cell-derived exosomes into non-malignant and malignant cells.* J Extracell Vesicles, 2016. **5**: p. 29877.
107. Nasiri Kenari, A., et al., *Proteomic and Post-Translational Modification Profiling of Exosome-Mimetic Nanovesicles Compared to Exosomes.* 2019. **19**(8): p. 1800161.
108. Schöneich, C., et al., *Apoptosis in differentiating C2C12 muscle cells selectively targets Bcl-2-deficient myotubes.* 2014. **19**(1): p. 42-57.
109. Yuste, V.J., et al., *The prevention of the staurosporine-induced apoptosis by Bcl-XL, but not by Bcl-2 or caspase inhibitors, allows the extensive differentiation of human neuroblastoma cells.* 2002. **80**(1): p. 126-139.
110. Chowdhury, R., et al., *Cancer exosomes trigger mesenchymal stem cell differentiation into pro-angiogenic and pro-invasive myofibroblasts.* Oncotarget, 2015. **6**(2): p. 715-31.
111. Cho, J.A., et al., *Exosomes from breast cancer cells can convert adipose tissue-derived mesenchymal stem cells into myofibroblast-like cells.* Int J Oncol, 2012. **40**(1): p. 130-8.
112. Dorsch, M., et al., *PK1/EG-VEGF induces monocyte differentiation and activation.* 2005. **78**(2): p. 426-434.
113. Leto, D. and A.R.J.N.r.M.c.b. Saltiel, *Regulation of glucose transport by insulin: traffic control of GLUT4.* 2012. **13**(6): p. 383-396.
114. Ramachandran, V. and R. Saravanan, *Glucose uptake through translocation and activation of GLUT4 in PI3K/Akt signaling pathway by asiatic acid in diabetic rats.* Hum Exp Toxicol, 2015. **34**(9): p. 884-93.
115. Mîinea, C.P., et al., *AS160, the Akt substrate regulating GLUT4 translocation, has a functional Rab GTPase-activating protein domain.* 2005. **391**(1): p. 87-93.

Abstract in Korean

엑소좀은 세포로부터 분비된 나노 소포체이며, 이는 세포 간 신호전달에서 중요한 역할을 담당하고 있다. 엑소좀은 서로 다른 세포 사이에 단백질, 지질, mRNA, miRNA 및 DNA 를 포함한 생체 분자를 전달하는 역할을 한다. 엑소좀은 생체 적합성, 안정성 및 낮은 면역원성을 통해 임상적 활용 가능성이 활발히 연구되고 있다. 그러나, 낮은 제작 수율, 이종성, 노동 집약적 제조 절차 및 치료적 로딩은 엑소좀의 임상 적용에 제약 요소로 제기되고 있다. 세포 유래 소포체는 천연 엑소좀에 비해 높은 생산성을 나타내며 생화학적 호환성으로 인해 엑소좀의 대안으로 간주되고 있으며, 이는 세포 유래 소포체의 임상 적용 가능성을 높여준다.

본 연구에서는 세포 유래 소포체를 통한 표적 막단백질 전달을 통해 근육 분화능이 상실된 세포의 근분화능 회복과 포도당 대사능의 회복 여부를 평가하였다. 이를 위한 개념 증명 연구로, 세포 유래 소포체를 이용하여 표적 세포로의 녹색 형광 단백질(GFP)의 전달을 평가하였다. GFP 를 도입한 인간 배아 신장 세포(*GFP*^{Tg} HEK293T)를 미세 압출하고, 회수된 세포 유래 소포체를 OptiPrep 밀도구배 초고속 원심분리를 통해 정제하여 GFP 가 함유된 고순도의 세포 유래 소포체(*GFP*^{Tg} CDVs)를 제작하였다. 10^7 개의 세포로부터 약 100 μg 의 *GFP*^{Tg} CDVs 가

제작되었으며, 세포 유래 소포체의 평균 직경은 약 173.1 nm 로 기존에 보고된 천연 엑소좀의 크기와 유사 하였다. 단백질 분석을 통해 *GFP*^{Tg} CDVs 는 CD9 및 CD81 과 같은 엑소좀 마커 단백질을 발현하고 있음을 관찰하였다. 또한, GFP 가 없는 일반 HEK293T 세포에 *GFP*^{Tg} CDVs 처리 후 30 분부터 세포에서 GFP 단백질 및 mRNA 가 성공적으로 검출되었고, GFP 의 발현은 해당 세포에서 최대 48 시간 동안 유지되었다.

이러한 결과에 기초하여, 세포 유래 소포체를 이용한 PROKR1 의 전달이 근분화능을 상실한 C2C12$^{Prokr1-/-}$세포의 분화 능력을 회복시킬 수 있는지를 확인하기 위해 약리 연구를 수행하였다. Prokr1 은 골격근의 대사 항상성에 중요한 유전자로, C2C12$^{Prokr1-/-}$ 근모세포는 근관으로 분화 될 수 없었다. PROKR1 을 과발현시킨 HEK293T 세포로부터 상술한 과정과 동일하게 제작된 *PROKR1*^{Tg} CDVs 는 평균 직경 161.7 nm 로 관찰되었고, CD9 및 CD81 을 포함한 표준 엑소좀 마커 단백질을 발현하였다. 또한, *PROKR1*^{Tg} CDVs 는 PROKR1 단백질을 함유하는 것을 확인하였고, PROKR1 단백질은 Prokr1 이 결손된 C2C12$^{Prokr1-/-}$ 근모세포에 성공적으로 전달되는 것을 관찰하였다. 세포 처리를 위한 *PROKR1*^{Tg} CDVs 의 농도는 MTT 분석을 통해 확인하였고, 세포 독성이 없는 *PROKR1*^{Tg} CDVs 의 최적 농도는 25 μg/mL 이하로

결정되었다. 근모세포 분화 후 출현하는 근아세포에서 *PROKR1*^{Tg} CDVs 에 의한 세포사멸 저해 효과는 유세포 분석을 통해 확인하였고, *PROKR1*^{Tg} CDVs 는 C2C12$^{Prokr1-/-}$ 유래 근아세포의 사멸을 8.4 % 수준에서 유의적으로 감소시키는 것을 밝혀냈다. *PROKR1*^{Tg} CDVs 는 C2C12$^{Prokr1-/-}$ 근아세포로부터 정상적인 C2C12 세포와 유사한 근관세포를 형성하였고, 해당 근관세포는 *Myh7, Mb* 및 *Myod* 등 근관세포 마커 유전자의 발현 향상 및 *Pax3, Pax7* 및 *Myod* 등 근모 및 근아세포 마커 유전자의 발현 감소를 나타내었다. 또한, *PROKR1*^{Tg} CDVs 로 유도된 C2C12$^{Prokr1-/-}$ 유래 근관세포는 정상적인 C2C12 세포 유래 근관세포와 유사한 수준의 인슐린 자극에 의한 포도당 흡수 반응을 나타내었다. 이러한 결과는 *PROKR1*^{Tg} CDVs 가 PROKR1 단백질을 C2C12$^{Prokr1-/-}$ 근모세포로 효율적으로 전달하고 결손된 근분화능을 회복시킬 수 있음을 의미한다.

결론적으로, 이러한 결과는 *PROKR1*^{Tg} CDVs 를 이용한 근육 질환의 치료 가능성 제시하고 있다. 또한, 형질전환 세포 유래 소포체는 활성 약리 성분을 전달하는 효과적인 수단으로 판단되며, 종래의 약제와는 차별화된 대체 치료제에 사용될 수 있다.

키워드: 세포 사멸, C2C12, 세포 유래 소포체, GFP, 포도당 흡수, 근분화, PROKR1

학생 번호: 2018-23506

Acknowledgements

Time is flying, and the two-year graduate career is about to end. Looking back on these two years, I thank my efforts. Of course, without the help of professors and classmates, I cannot complete my master's degree. For those who guide me, help me, and inspire me, I am very grateful.

Most important is my professor, 박중훈 교수님, during my studies as a graduate student, I deeply felt the care, kindness, and patience from Professor Park. From the topic setting of the thesis to the final writing, the professor has devoted a lot of effort. As a teacher, he always gave me guidance when I was confused. We have laboratory meetings every week, and students report and discuss experimental results and accept the professor’s suggestions. There is a journal meeting on Friday, papers in related fields will be presented. From paper, we study research methods and research thinking. I learned four lessons from my professor, include Topics in Assisted Reproduction Technology, Cellular Differentiation, Regulatory Toxicology and Nonclinical Studies. The professor is very knowledgeable, he knows a lot of proprietary biological terminology, some of words I have never heard about that. How poor my English is, I hope it can improve in the future.

As an elder, my professor cares about my life. He often urges me to go home quickly on Friday night and give me a good rest. On Sunday morning, he will take students to church. In the church, I have met many friends and I was very impressed by concert and outdoor games. There has one friend, her

name is 이주은, because she speaks Chinese very well, she tells me many interesting things and takes care of me a lot. I still remember when we first came to school, my professor gave us an overview of the school and majors. Nowadays, he often takes students out to relax and reduce the pressure on learning. Dinner, singing, climbing, picnic, movie all of these make me relax and happy. He taught students something truth at dinner. He asked me if I am used to eating Korean food, if I do sports or not. He cares my feeling I am really appreciating for that. I have received many cares from my professor in daily life. I feel so lucky to be my professor's student.

Then, I want to express my appreciation to university mentor, professor Hong Zhongshan, without him, I don't have this chance to be here. I will keep grace in my mind.

The person in my master experiment who helped me most is 목종수 선배님. He is a good helper for professors and a good leader for students. He is my experimental tutor. He taught me a lot of experimental techniques and told me the precautions for the experiment. We discussed the experiment and he adjusted his time to help me. I am very grateful to him in my heart. He takes care of me a lot during outdoor activities. Because I couldn't read Korean recipes, he asked me what I wanted to eat. He is so kind. I can't finish the experiment without his help. I will remember his help in my heart. 김은서 and 성연우 are my junior. They help me a lot in life. When I have something

confused, I will ask them. They care of me when we go outside and eat dinner. In Gangneung and Jeju Island, we had a happy time. Every time I stay in a hotel, I will envy their makeup techniques. Thank you for giving me a birthday, it's very warm.

I want to express my gratitude to 박태섭 교수님, He helped to generate transgenic cells. He helped me in the experiment, especially in FACs, operating the machine and analyzing the data.

In my impression, 염수청 교수님 and 김태민 교수님 are very kind, they always smile. Because they are in same track with our lab, so our three laboratories often get together to eat dinner and watch drama in Seoul. 김태민 교수님 is so kind, he often use his car to send students back to the student dormitory in night. He can speak Chinese. I have learned many things from his class. I take one class named Thesis Writing and Research Ethics from 염수청 교수님, it helped me a lot during my thesis writing. He is very earnest and responsible and wants students to understand, he teaches students to operate endnote on the computer one by one. He often buys fried chicken and pizza for us. He is a so good professor!

In the second floor of 102 building, 강상기 교수님 and 김종근 교수님 leave me a deep impression. I still remember when I came to school at first day, 강상기 교수님 said that this school is surrounded by mountains, there

is no place for entertainment, you have to study hard. I really like the style of his lessons. He always explains the principles clearly in simple words. 김종근 교수님 is very kind. He takes good care of students.

I also want to thanks to 지성태 교수님. He is very enthusiastic and caring. He often takes us out to eat delicious food. This Spring Festival, he ate hot pot together with Chinese students, and we went to KTV to sing. He is very attentive and always make slogan to celebrate the festival. He is so heart-warming.

Then, thanks to my Korean teacher 김고은, she is beautiful and wise. Thanks for 한영인 선생님, he teach me a lot about experiment. And he helps me a lot at early time. Thanks for 은비 언니 and 김학진 오빠, they sometimes take us out to buy food on Friday afternoon. 은비 언니 take us to Chuncheon to get the Alien registration card, and she helped me pay the first semester tuition fee with 호리나. Thanks to my roommate, she is nice and we eat delicious food together. Thanks to 한지선, 김서우, 조해진 and 조정현, they always make me feel happy and comfortable.

Fortunately, there are many Chinese friends around me, 조양, 호리나, 조국강, 유창, 왕신, 위승남, 이연분, 청혜린. When I was bored, sad, and helpless, they were by my side. We often eat fried chicken and chat together. During the

Spring Festival and Mid-Autumn Festival, we get together and make traditional Chinese food. On weekend, we went to Gangneung, Seoul, Wonju and other places. Chatting with them can release my pressure and make me happy and in a good mood. Sometimes, a sentence from them can prevent me walking into the corner of thinking.

My family has always been my infinite motivation to work hard. I thank them for their companionship and support along the way. A new life is about to start. I will work hard and make my parents proud of me.

Thanks to all of you! I feel very lucky to meet so many excellent and good people. It is my pleasure to have a good time with all of you in PyeongChang.

2020 년 6 월 18 일

장춘견 올림